

Nuclei Near and at the Proton Dripline

Marek Pfützner* and Chiara Mazzocchi

Abstract Nuclei in the vicinity of the proton dripline and beyond it are a fascinating realm within the chart of nuclei. In this chapter the main phenomena that characterise this domain and are not to be found elsewhere are explored. While moving away from the β -stability valley towards the proton dripline, phenomena like very exotic decay modes such as β -delayed (multi-) particle emission, and proton-, or two-proton radioactivity are encountered. Landmark nuclei are here two isotopes with magic proton and neutron numbers, ^{48}Ni and ^{100}Sn . Moreover, proton-rich nuclei ($N < Z$) display other interesting features, like breaking of isospin symmetry with consequent asymmetry in the energy spectra between mirror nuclei, the so-called Thomas-Ehrmann shift, or the phenomenon of proton-halo. Last but not least, nuclei close to the proton dripline play a very important role in nucleosynthesis, since they take part in the rapid-proton capture process and their properties are crucial in defining the flow followed and its termination close to ^{100}Sn .

1 Introduction

An atomic nucleus - a quantum object composed of Z protons (atomic number) and N neutrons - is held together by strong nuclear forces. For limited combinations of the Z and N numbers this object is stable or very long-lived - in nature there are less than 300 such nuclei. In laboratories, however, more than 3000 unstable, radioactive

C. Mazzocchi
Faculty of Physics, University of Warsaw, Pasteura 5, 02-093 Warszawa, Poland e-mail: chiara.mazzocchi@fuw.edu.pl

M. Pfützner
Faculty of Physics, University of Warsaw, Pasteura 5, 02-093 Warszawa, Poland, e-mail: pfitzner@fuw.edu.pl

* corresponding author

nuclei were synthesized so far, and this number is still growing due to constant progress of acceleration and detection techniques. This progress is motivated and reinforced by intense research activities devoted to study properties of nuclei as far as possible from stability, at the edges of nuclear binding. With increasing imbalance between Z and N numbers, new phenomena appear and new challenges arise for theories of nuclear structure and reactions.

In general, the body of the nuclear world, as represented on the chart of nuclei, has three frontiers. One corresponds to large mass numbers, $A = Z + N$. The range of superheavy nuclei is not yet known, but it is ultimately limited by fission. The second border stretches along most neutron-rich side of the chart. This chapter, however, focuses on the third frontier represented by the most proton-rich, and thus most neutron-deficient, nuclei. To be specific the most neutron deficient isotopes of all elements up to uranium are considered. This nuclear domain abounds with phenomena and features which either do not have counterparts at the neutron-rich side of the chart or differ from them significantly.

One of the most characteristic hallmarks here is the Coulomb interaction. From its interplay with nuclear forces, the Coulomb barrier emerges, which hinders the emission of unbound protons. As a result, even beyond the proton dripline, β decay competes with proton (p) or two-proton ($2p$) radioactivity and often dominates. Since the β -decay energies are large and separation energies for charged particles are small, various channels of delayed emission after β^+ decay are opened. The wavefunction of a weakly bound proton cannot extend as far as in the neutron-halo case due to the Coulomb barrier. On the other hand, the increased radius of s -proton states leads to energy reduction known as the Thomas-Ehrmann shift, which does not have an equivalent at the neutron-rich side. Important source of information on nuclear forces are nuclei along the $N = Z$ line, where protons occupy the same single-particle states as neutrons. This line, starting at stability for lightest systems, approaches the proton dripline with increasing mass number and crosses it around ^{100}Sn . This supposedly doubly-magic, $N = Z$ nucleus is an important testing point for the nuclear shell-model. Another doubly-magic candidate is ^{48}Ni , which is the most neutron-deficient nucleus known, having isospin projection $T_z = -4$. A lot of experimental efforts are still needed to study these extremely hard to reach exotic systems. Investigations of nuclei on both sides of the $N = Z$ line probe the nuclear mirror symmetry and shed light on the limitations and advantages of the concept of isospin in nuclei.

In this chapter a portrait of the fascinating territory of nuclei at the proton dripline is sketched. First, a global overview of the region will be given with the current status of the exploration. Then, the main methods used to produce proton rich nuclei will be briefly presented. Further, several phenomena and research topics specific to the proton dripline region will be described in more details.

All information on nuclear properties, where no specific reference is given, were taken from the ENSDF database (2022).

2 Landscape

The limits of nuclear existence are characterized by nuclear binding energies. The line separating nuclei bound by nuclear forces from the unbound ones is called the dripline which is defined by means of nucleon separation energies. Since here the proton-rich edge of the chart of nuclei is being discussed, the corresponding dripline is determined by the one-proton and two-proton separation energies:

$$S_p(N, Z) = B(N, Z) - B(N, Z - 1) \quad (1)$$

$$S_{2p}(N, Z) = B(N, Z) - B(N, Z - 2). \quad (2)$$

$B(N, Z)$ is the binding energy of the nuclide (i.e. the neutral atom) defined by:

$$M(N, Z) = ZM_H + Nm_n - B(N, Z)/c^2, \quad (3)$$

where $M(N, Z)$ is the nuclide mass, the M_H and m_n are masses of the hydrogen atom and the neutron, respectively, and c is the speed of light. Both separation energies decrease when moving from stability towards neutron deficient side along the line of isotopes with a given atomic number Z . Then, the proton dripline is located between the last isotope with the positive values of S_p and S_{2p} and the next one for which one of these separation energies becomes negative. It happens that for the odd- Z elements, the S_p energy dictates the position of the dripline, as it becomes negative first. However, for the even- Z , due to the pairing energy between protons, the S_p for the proton-rich systems is larger than the S_{2p} , thus the latter value settles the dripline location.

Nuclei beyond the proton dripline are proton-unbound, so they can spontaneously emit protons from the ground state, giving rise to one-proton or two-proton radioactivity. The nuclear potential for a proton-unbound nucleus is schematically presented in Figure 1. Although the last proton is unbound, it is confined by the Coulomb barrier which prevents it from rapid emission. The tunneling probability through this potential barrier is extremely sensitive to the height and the thickness of the barrier, thus, to the decay energy $Q_p = -S_p$. Only when this probability is large enough, the proton emission can win the competition with β^+ decay. The same argument applies to two-proton emission for even- Z nuclei. It follows that while the observation of proton (or two-proton) emission proves the nucleus to be located beyond the proton dripline, the position of this line, except for the lightest nuclei, cannot be determined from decay data alone. The exact position of the dripline can be deduced only from precise mass measurements of the nuclei.

For completeness, in the past also other definitions of the dripline were used, which were based on the half-life criterion or on the dominance of nucleon emission over β decay. The definition given above, based on separation energies, is presently most widely accepted and will be used throughout this article.

Theoretical modelling of the proton dripline is one of important probes for understanding of nuclear forces. A recent global prediction, obtained with an advanced modern method, is shown in Figures 2 and 3. The solid lines represent the proton

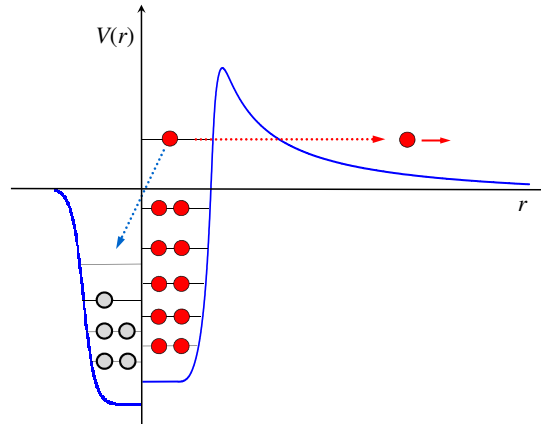


Fig. 1 Schematic representation of a proton-unbound nucleus. The blue solid line illustrates the radial part of nuclear potential as a function of the distance from the nuclear center (r). The potential felt by protons, represented by red circles, is shown on the right side. The sum of the repulsive, long range Coulomb interaction and the attractive, short range nuclear force creates the Coulomb barrier. The potential felt by neutrons (gray circles) is shown on the left. The dotted lines indicate alternative decay modes: p emission and β^+ decay.

dripline according to Neufcourt et al. (2020a,b) who applied the state-of-the-art nuclear density functional framework with several energy-density functionals to predict masses at the neutron-deficient edge of the nuclear chart. A novel feature of their approach was a Bayesian Model Averaging (BMA) analysis which improves the quality of mass predictions by including the available experimental information through machine learning techniques. In this way, the “collective” prediction of maximized accuracy, rooted in the current experimental knowledge, was obtained.

Figures 2 and 3 present also features and hallmarks of the proton dripline region which will be discussed in the following. The area in gray represents the nuclei which were observed, thus for which some experimental information is available. The established p - and $2p$ -emitters are indicated and their locations can be seen to be consistent with the predicted dripline. In contrast to the neutron-rich edge of the chart, the experimental reach is very close to the proton dripline for all elements and in many cases, mostly for odd- Z , it goes beyond. For example, the proton-radioactive, most neutron-deficient isotope of thallium known to date, ^{176}Tl , has seven neutrons less than the last bound isotope ^{183}Tl ! Similarly, the most neutron deficient isotopes of gold (^{170}Au), iridium (^{164}Ir), rhenium (^{159}Re), and thulium (^{144}Tm), all identified as proton emitters, are located six neutrons beyond the proton dripline. This is a result of the Coulomb barrier, which prevents a fast escape of unbound protons. How far it is possible to go with nuclear spectroscopy of proton-unbound nuclei depends on experimental limits of production, identification and de-

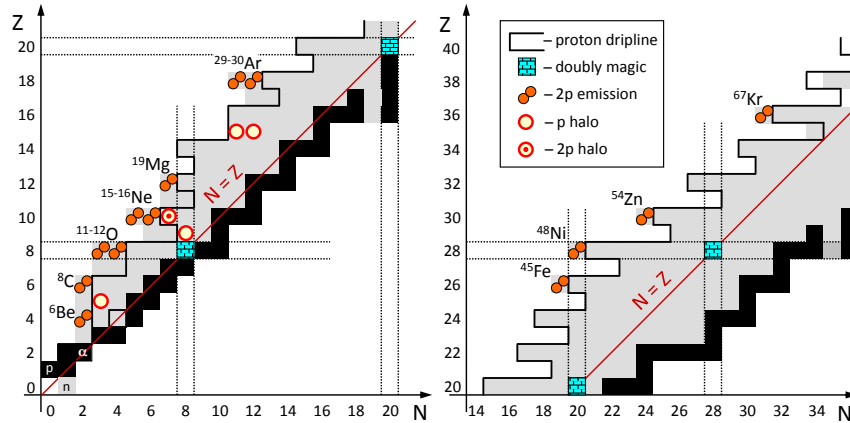


Fig. 2 Part of the chart of nuclei showing proton rich isotopes of elements below zirconium ($Z = 40$). Labels refer to nuclei decaying by ground-state $2p$ emission. The black squares mark the stable nuclei. Gray area denotes nuclei reached by experiments. The solid line represent the proton dripline prediction by Neufcourt et al. (2020a,b). Dotted lines show the position of magic numbers.

tection of the shortest half-lives. The reason why no proton emitters were observed yet below tin is just because of the lower Coulomb barrier their expected half-lives are too short for the current experimental techniques.

In the proton-rich landscape two special landmarks are ^{48}Ni and ^{100}Sn - nuclei with magic numbers of neutrons and protons, according to the classical shell model. Whether they indeed are doubly closed-shell systems is still a matter of studies and attracts a lot of interest, especially in view of growing evidence for shell evolution far from stability, as discussed by Otsuka et al. (2020). ^{48}Ni decays by $2p$ radioactivity (Pomorski et al. (2011b)) and it is believed that detailed studies of this decay mode may shed light on the structure of this nucleus. A support for the doubly magic character of ^{100}Sn was provided by Auranen et al. (2018) who observed the superallowed α decay chain $^{108}\text{Xe} \rightarrow ^{104}\text{Te} \rightarrow ^{100}\text{Sn}$, albeit still with extremely low statistics (two events!).

The appearance of α decay on the chart of nuclei is a more general indicator of increased binding due to closed shells. A little island of α -decaying isotopes of tellurium ($Z = 52$), iodine ($Z = 53$), and xenon ($Z = 54$), above ^{100}Sn , is the first manifestation of this effect. It happens again, more clearly, for neutron-deficient nuclei with $N \geq 84$. In fact, from this point α emission becomes the dominant decay mode along the proton dripline, only competing with proton radioactivity for the most exotic odd- Z nuclei.

The third crossing of magic lines, seen in Figure 3 (lower part) occurs at ^{164}Pb , which has 15 neutrons less than the expected last bound lead isotope. Unfortunately, this is much too far for any reasonable chance to consider it as a subject of nuclear physics studies.

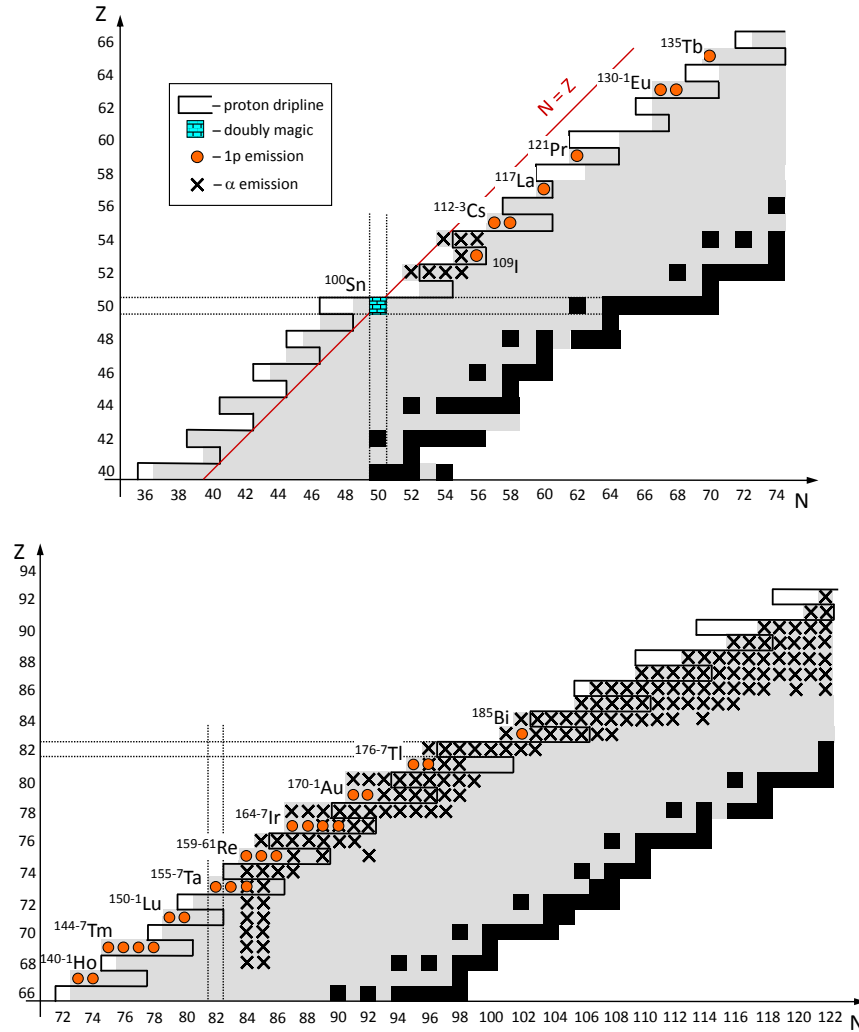


Fig. 3 Parts of the chart of nuclei showing proton rich isotopes of elements between zirconium ($Z = 40$) and uranium ($Z = 92$). Labels indicate the position of ^{100}Sn and nuclei decaying by p emission. Crosses mark nuclei for which the α emission is the dominating decay mode. Otherwise the same as in Figure 2.

3 Methods of production

The study of exotic nuclei at the proton dripline presents several challenges for the experimenter. It is intrinsic in the *exotic* term that such nuclei are likely short-lived and have very low production rates. Their production cross-section can be as low as

a few femtobarns with rates of the order of single ions/day (Kubiela et al. (2021)). In the laboratory, proton-rich isotopes can be produced by fusion-evaporation, fragmentation or spallation reactions, each of which has its optimum range of applications.

Heavy-ion fusion-evaporation reactions have been over the last decades a very effective production method for proton-dripline nuclei. Projectiles with energies close to the Coulomb barrier, typically between 2 and 6 MeV/nucleon, undergo complete fusion with a target nucleus, creating an excited compound nucleus (CN). Light particles (neutrons, protons, α particles,...) are evaporated from the CN and a residual nucleus is formed. Note that the CN is more neutron deficient than both the projectile and the target nuclei, because the β stability line turns towards neutron-rich side with increasing mass. In addition, the evaporation of neutrons is favored over charged particles, which in turn favours the production of ions more proton-rich than the CN itself. Typical beam intensities amount to several tens of particle nanoamperes (pnA), while target thicknesses to only a few hundreds of $\mu\text{g}/\text{cm}^2$ up to mg/cm^2 to allow for the reaction products to leave the target.

Projectile-fragmentation reactions at mid-to-relativistic energies are an alternative approach to fusion-evaporation for the production of exotic nuclei, in particular when a suitable projectile-target combination is not available. It can be pictured as a two-step process: the first step is the collision (abrasion), which removes nucleons from the overlap region. The remaining nucleons (or “spectators”) constitute the highly excited “pre-fragment”, which in the second phase of the process (ablation) de-excites via evaporation of particles (here again, the evaporation of neutrons is favored) and γ -ray emission. The so-called “Abrasion-Ablation” Model developed by Gaimard and Schmidt (1991) is based on such a view. Typical beams range from carbon to uranium at energies from 50 MeV/u to 1 GeV/u, while targets are of the order of g/cm^2 , 3–4 orders-of-magnitude thicker than those used in fusion-evaporation reactions, thanks to the larger beam energy. A key feature of this reaction is that projectile fragments, after escaping the target, move basically in the same direction as the projectile and with almost the same velocity. This allows for a fast transport of products to the detection station and facilitates formation of a radioactive beam.

Intense beams of exotic proton-rich isotopes can be obtained also by spallation reactions. In this process, an incident light particle (typically proton) at mid-to-high energy hits a target nucleus, and triggers a series of reactions: nucleons, light charged-particles (hydrogen and helium isotopes, pions, ...), and heavier (residual) nuclei are emitted, in addition to products of elastic and inelastic interactions of the projectile with the target. The residual nucleus is usually rather highly excited and will de-excite by emitting ejectiles and γ radiation. As a result, exotic nuclei are formed among the multitude of reaction products. The main advantage of this reaction is that beams of high-energy protons (0.5–1 GeV) with high current, up to 100 μA are readily available, and very thick targets can be used. A disadvantage is that the products are formed at low velocity and have to be extracted from the target.

The common denominator of these production mechanisms is the fact that a wide range of reaction products are generated, among which are the isotopes of interest. The latter, given their exotic nature, have production rates that are orders of mag-

nitude lower than those of the remaining (contaminant) isotopes. Such feature calls for selection of the ions of interest among the wealth of reaction products in order to study their properties. The selection (and identification) is achieved with the aid of electromagnetic fields according to the mass-to-charge ratio (A/q), which, for a particle of momentum p and charge q , is related to the magnetic field B via the relation:

$$\frac{A}{q} = \frac{p}{q} = \frac{B\rho}{\beta\gamma} \cdot \frac{e}{c \cdot u}, \quad (4)$$

where ρ is the radius of particle trajectory, β is the particle velocity in units of c , γ is the Lorentz factor $(1 - \beta^2)^{-1/2}$, e is the electron charge, and u is the atomic mass unit.

Two complementary methods are typically employed to select and identify exotic ions: in-flight separation and isotope separation on-line (ISOL). The in-flight separation is used together with fusion-evaporation and fragmentation reactions, in which reaction products emerge from the target with substantial velocity. From this stems one of the main features of this method - its speed. The time-of-flight of ions through the separator is of the order of $1 \mu\text{s}$ and such short half-lives can be accessed. The method is independent of the chemical properties of the ion studied. Ions of interest are selected by means of a combination of magnetic and electrostatic elements, such as dipoles, quadrupoles, sextupoles, Wien filters, etc. A crucial characteristic of the in-flight separation is the possibility of the full identification of ions that arrive to the end of the spectrometer on an ion-by-ion basis. Products of fusion-evaporation reaction are selected by a recoil separator. Examples of recoil separators are FMA at Argonne National Laboratory (Davids et al. (1992)) and RITU at Jyväskylä (Leino et al. (1995)). Products of fragmentation reaction are filtered by a fragment separator. Examples of fragment separators are the FRS at GSI (Geissel et al. (1992)), A1900 at the National Superconducting Cyclotron Laboratory (Morrissey et al. (2003)), LISE at GANIL (Mueller and Anne (1991)) and BigRIPS at RIKEN (Sakurai (2008)).

On the other hand, the ISOL method is usually used in conjunction with the spallation method. The reaction target is coupled to an ion-source. The reaction products are released from the target into the ion-source, ionised and extracted by means of a few tens of kV (typical 30-60 kV) acceleration potential. The separation of the ions according to their mass-to-charge ratio takes place in a uniform magnetic sector field, and the selected ions are directed to measuring station(s). In contrast to the in-flight separation, ISOL method is slow. The release times from the ion source range from tens to hundreds of ms, which limits the range of isotopes accessible. Nevertheless, in favourable cases, the ion-source can allow for additional selection of the ions of interest from the isobaric contaminants, thanks to its chemical sensitivity. Ion sources consist of a very hot cavity in which ionization proceeds through surface ionization, thermal ionization or interaction of the atom with a plasma. In some cases, better separation can be achieved by shining an appropriately tuned laser into the hot cavity of the ion source and exploiting the selectivity of laser resonance ionisation of atoms (Fedosseev et al. (2012)). Laser ionization is a powerful separation method to the level that it may allow to separate the ground state from an

isomeric state. Examples of ISOL facilities are IGISOL at Jyväskylä (Äystö (2001)), ISOLDE at CERN (ISOLDE), and ISAC-I at TRIUMF (ISAC).

Modern facilities couple a traditional first stage based on ISOL or in-flight separation with post-acceleration. Such combination allows to obtain beams of pre-selected radioactive species at higher energies and excellent ion-optical properties. This opens possibilities for a broader range of studies with good quality radioactive beams. Facilities of this type are, e.g. HIE-ISOLDE at CERN (HIE-ISOLDE) and ISAC-II at TRIUMF (ISAC).

Production, separation, and identification methods of exotic ions are discussed in greater detail elsewhere in this Handbook.

4 Decays of proton-rich nuclei

Along the path on the isobaric chain from stability towards and beyond the proton dripline, nuclear properties evolve and different phenomena appear. Nuclei west of the β -stability line are unstable against β^+ / EC decay, till the dripline is overcome, where other phenomena like proton and two-proton radioactivity manifest themselves. Along the path from stability to the dripline, once the $N = Z$ line is crossed, the Isobaric Analogue State (IAS) in the daughter nucleus falls within the Q_{EC} window. Both, the initial state and its IAS belong to the same isospin multiplet and thus have the same structure (as far as nuclear forces are concerned), so the Fermi transitions, which can occur only between IASs, become observable in β decay. A way to characterize β decay is to determine the so-called comparative half-life or ft -value, where f is the phase space integral that depends on the decay energy and Z (Wilkinson and Macefield (1974)) and t is the partial half-life for a given transition. The ft -value is related to the Fermi- and Gamow-Teller reduced nuclear matrix elements squared $B(F)$ and $B(GT)$ via the relation:

$$ft = \frac{K}{B(F) + (g_A/g_V)^2 B(GT)}, \quad (5)$$

where

$$K = \ln 2 \frac{2\pi^3 \hbar^7}{g_V^2 m_e^5 c^4} = 6144(4) \text{ s},$$

and g_V and g_A are the nuclear vector and axial-vector weak coupling constants, respectively (Hardy and Towner (2020)). Determination of the ft value, which depends on measured quantities, allows to extract the transition matrix elements to be compared with theoretical predictions, shedding light on the structure of the states involved. If the matrix elements can be calculated with sufficient precision, then the coupling constants can be calculated from measured quantities. A very important application of this idea is the high precision measurement of the g_V from $0^+ \rightarrow 0^+$ super-allowed Fermi transitions. It is used to test the Standard Model of fundamental interactions by checking the conserved-vector-current (CVC) hypothesis of weak

interactions and the unitarity of the Cabibbo-Kobayashi-Maskawa (CKM) matrix. A comprehensive survey of this research field is provided by Hardy and Towner (2020).

An important characteristic of the path leading from the stability valley to the proton dripline is the increasing of Q -values for β decay and simultaneous drop in the proton(s) separation energies, to the point where the latter will become negative at the dripline, as introduced in Section 2, see Figures 2 and 3. Such properties open the way to a “zoo” of exotic decay modes, ranging from β decay followed by emission of particles (delayed emission) to one- and two-proton radioactivities. Which β -delayed emission channels are opened depends on the energy of the daughter state fed in the β decay and on particle separation energies – in principle any combination of particles which is allowed energetically can be emitted. So far, for proton rich nuclei, delayed emission of one, two, and three protons (βp , $\beta 2p$, $\beta 3p$), as well as an α particle ($\beta\alpha$) and an α particle with a proton $\beta\alpha p$ were observed. The variety of decay channels of an exotic nucleus is illustrated in Figure 4. Investigating decay properties of so exotic nuclear systems can provide a wealth of information on nuclear structure of bound or weakly-bound systems.

In the following each of the main decay modes, characteristic for nuclei at or close to the proton dripline, is presented and illustrated with selected examples. Separate attention is given to the doubly-magic ^{100}Sn and the region around it, where the combination of having $N = Z$ and dripline proximity generates an island of α and proton decays.

More exhaustive and detailed discussion of exotic decays can be found in review papers by Blank and Borge (2008), Blank and Płoszajczak (2008), and Pfützner et al. (2012). A recent review of β -delayed proton and α emission can be found in Batchelder (2020) and the decay mechanisms are also extensively discussed in other parts of this book.

β -delayed charged particle emission

Over a century ago, Rutherford and Wood (1916) observed for the first time β -delayed particle emission, $\beta\alpha$ from ^{212}Bi , although correct interpretation of their findings came later by Gamow (1930). A few decades later, βp and $\beta 2p$ decays were also finally discovered (Barton et al. (1963); Cable et al. (1983)). All in all, since the discovery of β -delayed particle decay, about 200 βp emitters are known, some of which present branching ratios also for $\beta 2p$, $\beta 3p$, $\beta\alpha$ and $\beta p\alpha/\beta\alpha p$ (Batchelder (2020)).

Since βp stems from population in β^+/EC decay of excited states that are particle-unbound, its investigation offers a tool for probing the β strength distribution to particle-unbound states. Decays of nuclei close to the proton dripline, which have $N \leq Z$, have the IAS in the daughter nucleus located well above the particle(s) separation energies. For these nuclei, Fermi decay to the IAS will have a major contribution to the decay strength and the position of the IAS makes it open to emission of particles. For example most of the $\beta 2p$ emission cases known to date proceed in

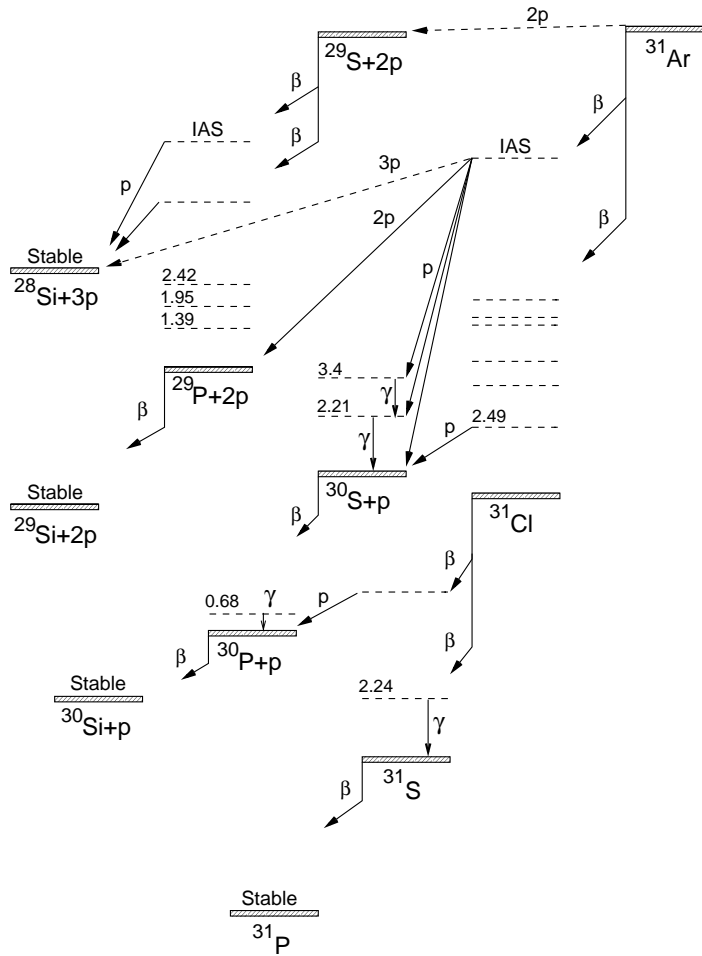


Fig. 4 Schematic representation of the possible decay paths for ^{31}Ar , highlighting the variety of decay channels of an exotic nucleus, as well as the richness of information that can be acquired by investigating such decay. Note that $\beta 3p$ decay channel of ^{31}Ar was reported by Koldste et al. (2014a) and by Lis et al. (2015). Figure from Jonson and Riisager (2001), Copyright (2001), with permission from Elsevier.

fact through the IAS, but contribution of Gamow-Teller transitions to higher excited states cannot not be neglected. The power of such investigations is well illustrated by the case of ^{31}Ar , one of the most studied β -delayed (multi-) charged-particle emitters, having a large decay energy $Q_{EC}=18.3(2)$ MeV, see Figure 4.

A detailed study by Fynbo et al. (2000) reported on the measurement of proton energies and angular correlations in the $\beta 2p$ decay of ^{31}Ar , showing that the decay mechanism is dominantly sequential, i.e. the interaction between the proton and the recoil nucleus determines the decay mechanism, rather than the proton-proton

interaction. Fynbo et al. (2000) also identified for the first time $\beta 2p$ channels from levels fed by Gamow-Teller transitions, with consequent impact on the β strength distribution.

Observation of $\beta 3p$ emission channel was much more difficult because a sizable branching ratio for this decay appears in nuclei which are hard to reach by experiment. In fact, the first observation of this channel was achieved with a very sensitive and efficient detector, developed mainly to study $2p$ radioactivity. The TPC-type detector with optical readout (Warsaw OTPC) was used in a study of $2p$ decay of ^{45}Fe , as discussed a bit later. In the same experiment, however, the β decay branches of ^{45}Fe were measured and among them the first evidence for the $\beta 3p$ decay was found with a surprisingly large branching ratio of 11(4)% (Miernik et al. (2007a)). Moreover, ions of ^{43}Cr were implanted into the detector as contaminants, and for them the $\beta 3p$ decay was observed as well with the branching ratio of $8(3) \times 10^{-4}$ (Pomorski et al. (2011a)).

^{31}Ar was considered as a candidate for $\beta 3p$ emission and only after several attempts (Bazin et al. (1992); Fynbo et al. (1999)) this decay mode was finally identified, again with the Warsaw OTPC detector (Lis et al. (2015)), see Figure 5a. With 13 events observed, the extracted branching ratio was $7(2) \times 10^{-4}$. This finding was confirmed by Koldste et al. (2014a,b) with a different technique, based on array of silicon detectors. In spite of its low probability, $\beta 3p$ decay contribution to the total β strength is far from negligible, as was shown by Koldste et al. (2014b). About half of delayed three-proton decays proceeds through levels above the IAS in the daughter ^{31}Cl and makes up for as much as 30% of the total Gamow-Teller strength observed. Koldste et al. (2014a) shed also some light into the decay mechanism, showing that the three protons are emitted mainly sequentially. This remains to date the only case of $\beta 3p$ decay studied to such an extent. The case of ^{31}Ar highlights the usefulness of complementary studies with different techniques, as well as the importance of measuring very weak, exotic decay channels to obtain complete information on the decay and in consequence on the structure of nuclei involved.

As exotic as $\beta 3p$, is $\beta \alpha p / \beta p \alpha$ decay. The two descriptions for the latter reflect the fact that in case of a sequential decay, this process has two different paths: either the α particle is emitted first and followed by the proton, or vice versa. To date, this rare decay mode has been observed only in three isotopes, ^9C (Gete et al. (2000)), ^{17}Ne (Chow et al. (2002)) and ^{21}Mg (Lund et al. (2015)). Among these, ^9C is a special case, since all states populated in β decay disintegrate into a proton and two α particles via the $p+^8\text{Be}$ and $\alpha+^5\text{Li}$ channels. For ^{17}Ne , both $\beta \alpha p$ and $\beta p \alpha$ were observed, with a total branching ratio of $1.6(4) \cdot 10^{-4}$, while the total branching ratio for ^{21}Mg was found to be $1.6(3) \cdot 10^{-4}$. It is interesting to notice that the known $\beta \alpha p / \beta p \alpha$ proceed through α -conjugate nuclei, ^8Be , ^{16}O and ^{20}Ne . In their work, Lund et al. (2015) attributed the appearance of these rare decay modes to the variation of decay energy caused by odd-even effects, rather than clustering, as suggested by the path through α -conjugate nuclei.

Proton decay

Proton radioactivity was discovered over 50 years ago by Jackson et al. (1970) with the observation of protons emitted from an isomeric state of ^{53}Co and about a decade later, ground-state proton emission was discovered in ^{151}Lu and ^{147}Tm by Hofmann et al. (1982) and Klepper et al. (1982), respectively. To date, more than 40 proton emitters are known (including decays from isomeric states), as shown in Figure 3 and summarised in the most recent study of proton systematics by Delion and Dumitrescu (2021). The latter work shows that there is a linear dependence of the logarithm of the centrifugal-barrier-corrected decay-width from the Coulomb probability multiplied by the proton-formation probability, in a similar way to the Geiger-Nuttall law for α decay.

Proton radioactivity originates from the tunnelling of the proton through the barrier (see Figure 1) and its probability depends strongly on the barrier height and width seen by the proton, hence on its energy and angular momentum ℓ . Moreover, it is very sensitive also to the wave function of the initial and final states involved in the decay. A unique insight into the structure of proton-unbound nuclei is therefore obtained by measuring proton energies, half-lives and branching ratios. Moreover, the proton energy, corrected for the recoil, gives a direct measurement of the proton separation energy: this is usually the first (and often the only) method to obtain experimental information on the binding energy of nuclei beyond the proton dripline.

Details of nuclear structure play a very important role in proton decay and small fractions of the wave-function sometime have large impact on the decay. Another important aspect is that the majority of proton emitters are deformed nuclei and cannot be described by a simple spherical single-particle scenario. More complex wave functions are involved, with several components, of which only few play a role in proton emission. In particular, proton-decay probabilities can be smaller than they would under the assumption of a spherical potential.

An interesting example in this context is the decay of the proton emitter ^{145}Tm , which presents fine structure in its decay. The observation of fine structure is a powerful tool, since it provides additional insight into the wave function of the states involved in the decay. In their work, Karny et al. (2003) studied the proton radioactivity of ^{145}Tm and discovered proton transitions to the ground state and to the first excited 2^+ state in ^{144}Er . The branching ratio for the latter was found to be $(9.6 \pm 1.5)\%$. An analysis of the wave function of ^{145}Tm with a particle-core vibration model showed that it is dominated by the $\pi 1h_{11/2} \otimes 0^+$ component (56%), while the fine structure transition is due only to a small fraction of it, the 3% $\pi 2f_{7/2} \otimes 2^+$ component.

Two-proton decay

When an even- Z nucleus is beyond the proton dripline and its proton separation energy is still positive or very small, two protons can be emitted simultaneously while the emission of one proton is energetically blocked or strongly suppressed.

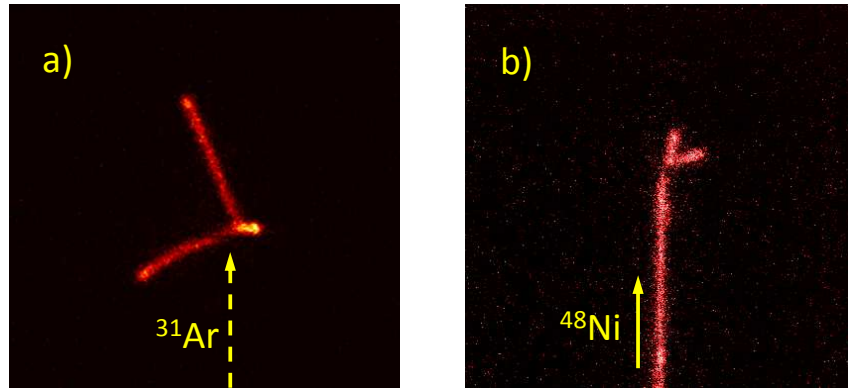


Fig. 5 Example CCD images recorded by the Warsaw OTPC detector; a) An event of β -delayed three-proton emission from ^{31}Ar . The track of incoming ^{31}Ar ion is not seen, as the CCD exposure was started after the ion implantation. b) Two-proton radioactivity of ^{48}Ni . Here the implanted ion entered during the exposure and its track is visible.

The possibility of such process of $2p$ radioactivity was first noted by Zeldovich (1960) and then examined in more detail by Goldansky (1960). The $2p$ emission was observed quite early for light nuclei, which were relatively easy to produce. The first cases studied were ^6Be (Geesaman et al. (1977)), ^{12}O , and ^{16}Ne (KeKelis et al. (1978); Kryger et al. (1995)). Because of the low Coulomb barrier in these nuclei they decay so fast that their ground states are characterised by the width rather than half-life - for example the decay width of ^6Be is about 100 keV. Such decays belong to the category of resonant phenomena and were dubbed *democratic* decays by Bochkarev et al. (1984).

The first observation of $2p$ radioactivity from a long-lived nuclear ground state occurred about 40 years after the first considerations of Zeldovich and Goldansky. It was achieved for ^{45}Fe in two experiments employing projectile fragmentation of a ^{58}Ni beam by Pfützner et al. (2002) and by Giovinazzo et al. (2002). The key factor in this breakthrough was the full identification of single ions arriving to the detection setup, which is one of the crucial advantages of the high-energy fragmentation method. In both experiments ions of ^{45}Fe were implanted into silicon detectors and the evidence of the $2p$ decay came from the measured total decay energy ($Q_{2p} \approx 1.2$ MeV) and the decay time ($T_{1/2} = 2.6$ ms). The same technique was used later by Blank et al. (2005) to discover $2p$ radioactivity in ^{54}Zn ($T_{1/2} = 1.6$ ms) and by Goigoux et al. (2016) to establish this decay mode in ^{67}Kr ($T_{1/2} = 7.4$ ms).

To detect directly and separately both emitted protons in order to measure the momentum correlations between them, which carry the information about the mechanism of the $2p$ decay, a different detection technique was adopted. It was based on the gaseous time-projection chamber (TPC) idea. In a TPC, the charged particles ionize the gas along their tracks and the freed electrons drift with a constant veloc-

ity in a uniform electric field towards a amplification region, after which they are detected. One such detector (Blank et al. (2010)) was used in the first, direct detection of two protons emitted in the decay of ^{45}Fe by Giovinazzo et al. (2007) and later in the study of $2p$ decay of ^{54}Zn by Ascher et al. (2011), but only seven events could be fully reconstructed.

In another, novel approach the TPC signal is read out by optical sensors, including a CCD camera. This optical TPC (Warsaw OTPC) was used in a detailed study of $2p$ radioactivity of ^{45}Fe by Miernik et al. (2007b). About 90 $2p$ decay events were recorded and fully reconstructed in three dimensions. The determined correlation pattern was found to be in a very good agreement with predictions of the 3-body model developed by Grigorenko and Zhukov (2003). Two important conclusions followed from this work. First, the essentially 3-body character of $2p$ emission was confirmed, which means that this process cannot be approximated by a sequence of two-body decays. Second, the correlation pattern seems to depend on the composition of the wave function of the initial nucleus, thus offering an insight into its structure.

In another experiment, the Warsaw OTPC was used by Pomorski et al. (2011b, 2014) to discover the $2p$ radioactivity of ^{48}Ni ($T_{1/2} = 2.1$ ms). An example CCD image of a $2p$ decay of ^{48}Ni is shown in Figure 5b. Since only four such decay events were recorded, no conclusions concerning the structure of this, supposedly double-magic, nucleus could be drawn. It is expected, however, that future experiments on ^{48}Ni ($Z = 28$) and on ^{54}Zn ($Z = 30$) will provide data with larger statistics and in connection with results for ^{45}Fe ($Z = 26$) will shed light on the $Z = 28$ shell closure at the proton dripline.

All $2p$ emitters observed below iron, shown in Figure 2, have so short half-lives that there is no time to identify them before they decay. They are produced in the reaction of a radioactive beam with a secondary target and they decay essentially at the same place, in-flight. The $2p$ decay is identified by detection of all the decay products and by the kinematical reconstruction. An example of such approach, to study $2p$ emission from ^{16}Ne , ^{19}Mg , ^{29}Ar , and ^{30}Ar , is described by Mukha et al. (2015, 2018).

Using the two-neutron knockout from a ^{13}O beam followed by invariant-mass spectroscopy of $2p$ decay products, Webb et al. (2019) observed broad states of ^{11}O . The measured spectrum was well fitted with the prediction of the Gamow coupled-channel model, including the $3/2^-$ ground state and three excited states. An interesting point is that ^{11}O is the mirror to famous two-neutron halo ^{11}Li . The ground state configurations of both nuclei were found to be similar.

A spectacular nuclear decay was observed for ^8C by Charity et al. (2011). This very exotic carbon isotope was produced by a neutron knock-out reaction from a beam of ^9C , followed by detection of all decay products. A sequence of two $2p$ decays, through the ground state of ^6Be was found, thus a 5-body decay!

¹⁰⁰Sn and its neighbourhood

A very special place in the chart of nuclei is taken by the doubly-magic ¹⁰⁰Sn, which is the heaviest self-conjugate nucleus being also bound against particle emission. The next $N = Z$ nuclides in the sequence, ¹⁰⁴Te and ¹⁰⁸Xe are in fact α emitters and predicted to lie beyond the proton dripline. The fact that ¹⁰⁰Sn sits so close to the proton dripline and is expected to be doubly magic, impacts not only the nuclear structure of the region, but also the path followed by the rp-process, see Section 7. Evidence of its doubly magic character is provided by theoretical predictions as well as by a series of properties of its decay and of the decay of its neighbours (Faestermann et al. (2013)). Here the main characteristics of this very special nucleus are summarized.

From a classic shell-model perspective, the $N = Z = 50$ ¹⁰⁰Sn has $\pi g_{9/2}$ and $\nu g_{9/2}$ orbitals filled up, while the $\pi g_{7/2}$ and $\nu g_{7/2}$ are empty. Therefore, in a pure single-particle picture, its Gamow-Teller β decay $\pi g_{9/2} \rightarrow \nu g_{7/2}$ will feed 1^+ states in the daughter ¹⁰⁰In, with dominant, very strong decay to one 1^+ state. The latter is the so-called *super-allowed* Gamow-Teller decay.

The first identification of ¹⁰⁰Sn was achieved by Schneider et al. (1995) and Lewitowicz et al. (1995). Hinke et al. (2012) studied the decay of ¹⁰⁰Sn in more detail and measured the half-life and determined the Q_{EC} by means of β end-point energy. They found the fastest β decay observed to date, with a record-low value for the $\log(ft)$. In a recent experiment, the decay of ¹⁰⁰Sn was reinvestigated by Lubos et al. (2019) with 10 fold more statistics and more accurate values for half-life and Q_{EC} were established, leading to the revised values $\log(ft) = 2.95(8)$, $B(GT) = 4.4^{+0.9}_{-0.7}$, which are still record low and high, respectively, in the whole chart of nuclei.

A signature of the doubly-magic character of ¹⁰⁰Sn combined with its proximity to the proton dripline is the appearance of an island of proton and α radioactivity just above it. Pioneers on this topic were Macfarlane and Siivola (1965), who observed for the first time α decay in the region and concluded that “*these nuclei represent the first opportunity to study alpha decay from nuclei where the “valence“ neutrons and protons are in the same single-particle level, in this case the $1g_{7/2}$ level. This may give rise to a kind of “super-allowed” alpha decay resulting in large reduced alpha widths.*”. Alpha decay studies of nuclei above ¹⁰⁰Sn can indeed not only provide evidence for the super-allowed α decay and consequently double magicity of ¹⁰⁰Sn, but also a deeper insight into shell evolution along the tin isotopic chain, when fine structure is observed, in a similar fashion to what is achieved in proton decay studies.

Studies of fine structure in α decay can shed light on the wave function of the levels involved in the decay and allow to determine their spin/parity. Of particular relevance is fine structure in the α decay of odd-A neutron-deficient tellurium isotopes. Several studies looked at odd-mass xenon-tellurium-tin decay chains as well as directly at tellurium-to-tin decays (Liddick et al. (2006); Darby et al. (2010); Seweryniak et al. (2002, 2006, 2007)). Fine structure in α decay will populate most likely the lowest-lying excited state in the daughter nucleus, given the dramatic dependence of the decay probability on the transition energy. The observation of such phenomenon can therefore allow to determine the position of the first excited state

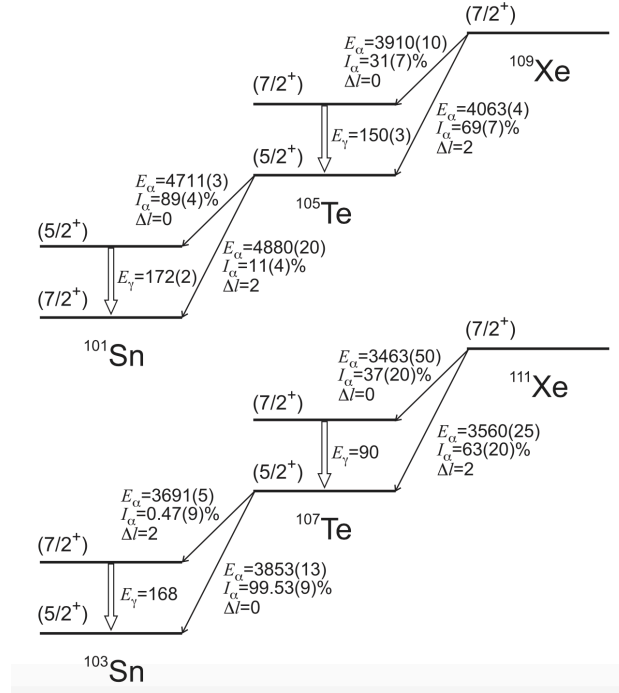


Fig. 6 α -decay chains $^{109}\text{Xe} \rightarrow ^{105}\text{Te} \rightarrow ^{101}\text{Sn}$ (Top) and $^{111}\text{Xe} \rightarrow ^{107}\text{Te} \rightarrow ^{103}\text{Sn}$ (bottom). Energies (E_α) in keV, intensities (I_α) and angular momentum carried in the decay (Δl) are shown for each transition, illustrating how spin/parity assignments were obtained. Note the inversion of levels between ^{103}Sn and ^{101}Sn . Figure from Darby et al. (2010). Copyright (2010) by the American Physical Society.

and combined with the branching ratio lead to the determination of the spin/parity of the levels involved. In particular, the decay of ^{105}Te to the first excited state in ^{101}Sn allows to determine the energy separation of the $vd_{5/2}$ and $vg_{7/2}$ orbitals (Seweryniak et al. (2006, 2007)), while fine structure in the decay allows to determine the order of the orbitals. Darby et al. (2010) observed fine structure in both the decays of the $^{109}\text{Xe} \rightarrow ^{105}\text{Te} \rightarrow ^{101}\text{Sn}$ decay chain, leading to levels positioning with a $(7/2^+)$ ground state and a $(5/2^+)$ first excited state in ^{101}Sn , see Figure 6. This observation indicates a surprising inversion of single-particle orbitals just next to the doubly-magic ^{100}Sn .

Super-allowed α decay will manifest itself with an α width

$$\delta_{\alpha}^2 = h \cdot \frac{\lambda_{\alpha}}{P}, \quad (6)$$

much larger than that for the corresponding valence nucleus in the ^{208}Pb region, the reference for α decay being $^{212}\text{Po} \rightarrow ^{208}\text{Pb}$ (Varga et al. (1992)), which till recently was the only α decay to a doubly magic nucleus known. Here λ_{α} is the partial decay constant and P the barrier penetration probability. The α width relative to that of ^{212}Po , $\delta_{\alpha}^2/\delta_{^{212}\text{Po}}^2$, is also called reduced α -decay width. (Much) larger-than-one values of the reduced α -decay width have been observed along the decay chains ending in magic neutron-deficient tin isotopes $^{114}\text{Ba} \rightarrow ^{110}\text{Xe} \rightarrow ^{106}\text{Te} \rightarrow ^{102}\text{Sn}$ (Mazzocchi et al. (2002); Capponi et al. (2016)) and $^{109}\text{Xe} \rightarrow ^{105}\text{Te} \rightarrow ^{101}\text{Sn}$ (Liddick et al. (2006); Darby et al. (2010)). However, the largest value of reduced width (hence α preformation probability) is expected for the decay of ^{104}Te leading to ^{100}Sn and indeed, an enhancement of a factor of at least 3 was observed in the decay width of ^{104}Te with respect to ^{212}Po (Auranen et al. (2018)). It should be noted that the latter result stems from a statistics of only two events and no clear evidence for the α decay of ^{104}Te could be found in a separate experiment by Xiao et al. (2019), calling for further studies with improved statistics. The data available to date on α decay close to ^{100}Sn have been recently re-analysed in the context of a superfluid tunnelling model by Clark et al. (2020), showing that for nuclei just above ^{100}Sn the α preformation probability is significantly larger than for those just above ^{208}Pb .

Last but not least, another phenomenon that is predicted to happen as a consequence of the double shell closure at ^{100}Sn is that of cluster radioactivity, similarly to what happens in the ^{208}Pb region (Bonetti and Guglielmetti (2007)), with the most promising candidate being ^{12}C emission in the decay $^{114}\text{Ba} \rightarrow ^{102}\text{Sn}$. After a first indication of this very rare decay mode to exist, a follow up measurement did not confirm the original results and only an upper limit of $3.4 \cdot 10^{-5}$ could be inferred for the branching ratio (Guglielmetti et al. (1995, 1997)). Since the partial half-life for this very rare decay mode is extremely sensitive to the Q -value, its precise determination can help constrain the expected half-life. An experimental value for $Q_{^{12}\text{C}}$ was determined from the observation of the $^{114}\text{Ba} \rightarrow ^{110}\text{Xe} \rightarrow ^{106}\text{Te} \rightarrow ^{102}\text{Sn}$ decay chain (Mazzocchi et al. (2002); Capponi et al. (2016)) yielding a partial half-life 4-7 orders of magnitude above the experimentally established lower limit of 1.2×10^4 s (Guglielmetti et al. (1997)). Though, the ideal candidate for observation of ^{12}C emission in this region is ^{112}Ba , which would decay to ^{100}Sn . Although ^{112}Ba production seems to be beyond the possibilities of present-day facilities, it should be within the reach of the next generation laboratories.

5 Isospin Symmetry

One of fundamental principles of nuclear physics is that to a good approximation the strong nuclear two-body interactions are charge symmetric and charge independent. The former means that strong proton-proton interaction equals the neutron-neutron

interaction and the latter extends this equality also to the proton-neutron interaction. The consequence of this symmetry is the isospin quantum number, which should be conserved by strong nuclear forces. Obviously the isospin symmetry is broken by the Coulomb repulsion between protons and other differences between the proton and the neutron, like mass or magnetic moment. The challenge is to identify and comprehend all the isospin-breaking effects. In turn, once these phenomena are understood, the isospin symmetry arguments can be applied to predict properties of unknown nuclei and anticipate regions of interesting processes on the nuclear chart. That is why the studies of isobaric spin (isospin) symmetry become an important research field in itself.

In this section a few illustrating examples from the research on isospin symmetry which involve very proton-rich nuclei are given. The discussion will be limited to pairs of mirror nuclei, where by mirror the interchange of Z and N numbers is meant. How asymmetry in mirror β decays can unveil structural differences between proton-rich nuclei and their reflections on the other side of the $N = Z$ line will be mentioned in Section 6, dedicated to proton halos.

Mirror symmetry

According to the charge symmetry, a nucleus and its mirror should have an identical set of states, having the same spins and parities, and similar excitation energies. As a result almost all known pairs of mirror nuclei have the same spin and parity in the ground state. There are only two known exceptions to this rule. One is the mirror pair ${}^{16}_9\text{F}$ - ${}^{16}_7\text{N}$. The ground state of ${}^{16}\text{F}$, which is proton unbound, is 0^- , while that of ${}^{16}\text{N}$ is 2^- . There is an excited 0^- state in ${}^{16}\text{F}$ at 120 keV, which indicates that there is an inversion of states between these two nuclei.

Very recently a second case was found for the pair ${}^{73}_{38}\text{Sr}$ - ${}^{73}_{35}\text{Br}$ by Hoff et al. (2020). The ground state of ${}^{73}\text{Br}$ is $1/2^-$ and it has an excited state $5/2^-$ only at 27 keV. In the decay spectroscopy of the very proton-rich ${}^{73}\text{Sr}$, which is one neutron away from the dripline, β decay to the IAS in ${}^{73}\text{Rb}$, followed by emission of delayed protons was measured. Two branches of proton emission were identified, proceeding to the ground state (0^+) and to the first excited state (2^+) in ${}^{72}\text{Kr}$. From the observed intensities of these two proton transitions, and with help of nuclear structure calculations using Gamow coupled-channels model (Wang et al. (2017)), the authors concluded that the spin of the IAS must be $5/2^-$, therefore, the ground state of ${}^{73}\text{Sr}$ must be also $5/2^-$. This is the first breakdown of the mirror symmetry between ground states of bound nuclei. Although it still needs to be confirmed, best by a direct measurement of the ground-state spin of ${}^{73}\text{Sr}$, the inversion of $1/2^-$ and $5/2^-$ states between ${}^{73}\text{Sr}$ and ${}^{73}\text{Br}$ was well reproduced theoretically. Lenzi et al. (2020) used large-scale shell model calculations taking into account the Coulomb interaction and also an isospin-breaking interaction of nuclear origin, which was introduced phenomenologically. It was found that the Coulomb interaction plays a dominant role in the observed inversion, and in fact it would suffice alone to explain the effect. Nevertheless, room for a small nuclear contribution was also admitted.

The approach used to explain the state inversion in the $^{73}\text{Sr} - ^{73}\text{Br}$ system was developed originally for the detailed analysis of energy differences between isobaric multiplets of high-spin states. It was used very successfully to study the influence of deformation, alignment, and intrinsic single-particle configurations on the mirror energy differences as a function of spin. Bentley and Lenzi (2007) summarized this extensive work, focused mainly on nuclei in the $f_{7/2}$ shell, for which experimental data for many excited states, up to high spins, were available and which were still within the scope of the large-scale shell model. One of the interesting finding in this program, reported by Zuker et al. (2002), was that the isospin non-conserving interactions of nuclear origin are at least as important as the Coulomb potential. This type of studies may bring important new results on the breaking of isospin symmetry when excited states of heavier nuclei, including very proton-rich mirror partners, will come within reach of experiment and large-scale shell-model analysis.

In a few regions of neutron-rich nuclei far from β stability changes of nuclear structure have been observed, exemplified by disappearance of classical shells and emergence of new ones. A comprehensive summary of these shell evolution phenomena was given recently by Otsuka et al. (2020). One example is the *island of inversion* around ^{32}Mg which is related to the weakening of the $N = 20$ shell closure. By mirror symmetry one could expect corresponding structural changes in very neutron deficient calcium isotopes ($Z = 20$). To probe this idea, Doornenbal et al. (2007) investigated the mirror pair $^{36}\text{Ca} - ^{36}\text{S}$. Employing the in-beam γ spectroscopy with the ^{37}Ca beam, they determined the energy of the first 2^+ state in ^{36}Ca , which was found to be 276 keV lower than its mirror in ^{36}S . This large asymmetry was interpreted as a result of shifts in the single-particle energies and was found consistent with the expectation that indeed calcium isotopes may develop another island of inversion for $N < 16$. Shell-model analysis of this case was extended by Valiente-Dobón et al. (2018) to the excited 0^+ state of intruder type, i.e. formed by 2 particles - 2 holes excitations. Such state is known in ^{36}S at 3346 keV. The calculations reproduced well the observed difference between 2^+ states and predicted a much larger asymmetry for the intruder 0^+ states - in ^{36}Ca it should be located 720 keV lower than in ^{36}S . In fact, it is expected to be the first excited state in ^{36}Ca decaying by $E0$ transition to the ground state. Thus, perspectives of further studies in the dripline region around $Z = 20$ appear attractive, although the mirror of ^{32}Mg , ^{32}Ca , is probably too far beyond the dripline (3 neutrons), to be reached by experiment.

Thomas-Ehrman shift

One reason for an energy shift between mirror states is the increased radial extent of the weakly bound valence proton in the $s_{1/2}$ orbit. Levels with significant contribution of this component are expected to experience smaller Coulomb repulsion and thus to be more bound (have lower energy) than their neutron-rich mirror partners. For example, the first excited state in ^{13}N ($1/2^+$ at 2365 keV) is 724 keV lower than its mirror in ^{13}C . This difference was analysed for the first time by Ehrman

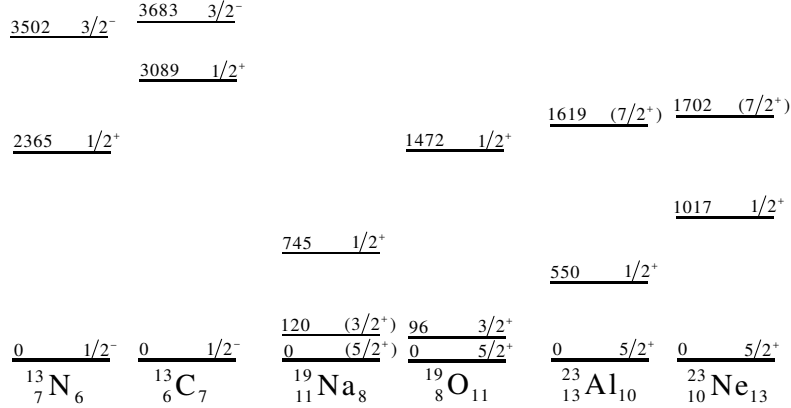


Fig. 7 Partial level schemes of three pairs of mirror nuclei illustrating the Thomas-Ehrman shift. Note that the largest energy difference occurs for $1/2^+$ states - their energy is lower in the proton-rich nucleus. Energy values are in keV.

(1951) and Thomas (1952), after whom the effect is named the *Thomas-Ehrman shift* (TES).

The TES was observed in a few other nuclei where the proton $s_{1/2}$ orbital plays an important role. Three prominent examples are shown in Figure 7.

Recently a modern shell-model hamiltonian for the sd shell was developed by Magilligan and Brown (2020), which incorporates isospin-breaking interactions. In addition, the authors examined a model of the TES. First, they calculated how the difference in proton and neutron $2s_{1/2}$ single-particle energies, relative to the difference in $1d_{5/2}$ energies, depend on the proton separation energy. Results for a ^{16}O core were found very similar to those with a ^{28}Si core, so a single curve, shown in Figure 8 left, was adopted as a model of the single-particle TES. This, together with the calculated proton $2s_{1/2}$ spectroscopic factors, allowed them to determine the energy shift of levels in several nuclei having $s_{1/2}$ components. The results of this procedure showed good agreement with experimental values, see Figure 8 right.

Originally, the mechanism of TES was invoked to describe a change of motion of a single nucleon. The underlying idea, however, can be extended to groups of nucleons, like clusters. For example α -clusters do appear in the structure of excited states in light nuclei, especially close to the threshold for α emission. In such case the nucleus can be viewed as a weakly coupled system of an α -cluster and the residual nucleus. Usually the wave function of the relative motion of these two parts has a large s -wave component and a difference due to Coulomb interaction should be observed for the mirror systems. This idea was applied by Ito (2016) to the mirror pair $^{10}\text{C} - ^{10}\text{Be}$, which can be described as two α particles and two nucleons. The calculation of the 0^+ states in these nuclei showed indeed significant energy reduction of states in ^{10}C which had dominant s -wave component. Similar conclusions were made by Nakao et al. (2018) for the $^{18}\text{Ne} - ^{18}\text{O}$ pair which were considered in the

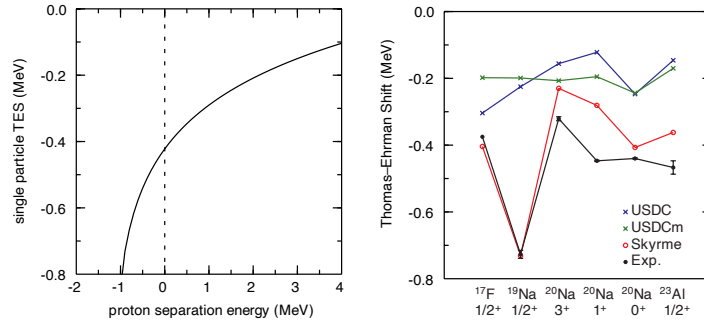


Fig. 8 Left: Calculated Thomas-Ehrman shift of the single-particle, valence $s_{1/2}$ proton orbit as a function of proton separation energy. Right: measured Thomas-Ehrman shift for the levels indicated (black, full circles), compared with shell-model predictions; the model including TES is labeled Skyrme (red open circles). See text for more details. Taken from Magilligan and Brown (2020), Copyright (2020) by the American Physical Society.

cluster model as $\alpha + ^{14}\text{O}$ and $\alpha + ^{14}\text{C}$ systems, respectively. The need to verify these predictions will hopefully motivate experimental activity in the field of clustering phenomena.

6 Proton halos

The phenomenon of a nucleon halo occurs when, due to a very low binding energy, one or two nucleons are able to tunnel far away from the nuclear binding potential. The resulting large spatial extension is one of the main characteristic features of a halo state. The neutron halo physics started from the discovery by Tanihata et al. (1985) of the large radius of the ^{11}Li nucleus. Soon it developed into an important and broad research field for neutron-rich nuclei and it is extensively discussed in other parts of this Handbook. Analogous phenomena are expected also for weakly bound proton-rich nuclei. Due to the Coulomb barrier, however, the halo effects are less pronounced and thus more difficult to investigate. Nevertheless, the one-proton- or two-proton-halos are expected for low Z nuclei with weakly bound valence protons in s - or p - states. Here a few, most pronounced cases, are presented.

^8B

The first case established as proton halo, and also the most intensely studied is ^8B . It has a very low proton separation energy, $S_p = 136$ keV. It appeared first as a halo candidate when Minamisono et al. (1992) measured a large quadrupole moment (Q) of ^8B , in fact twice larger than shell-model predictions. This result was found to be in agreement with the assumption of increased charge root mean square radius.

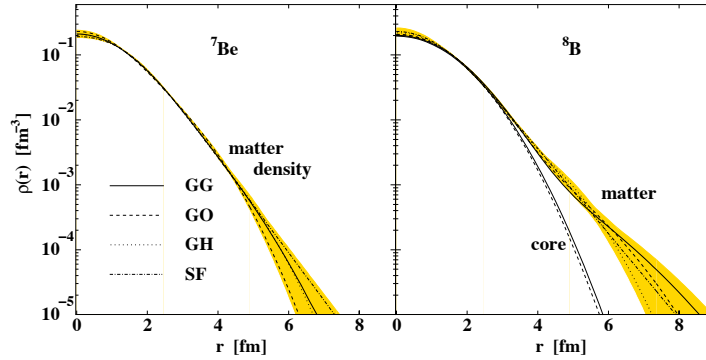


Fig. 9 Nuclear matter density distributions for ${}^7\text{Be}$ and ${}^8\text{B}$ deduced from the experimental data. The ${}^8\text{B}$ nucleus was assumed to consist of a ${}^7\text{Be}$ core and a loosely bound valence proton. The yellow error-bands represent envelopes of the density variation within the four parametrizations of density distributions considered, superimposed by the statistical errors. Reprinted from Dobrovolsky et al. (2019), Copyright (2019), with permission from Elsevier.

Although the large value of the Q moment is not a sufficient evidence for the halo structure, as noted by Nakada and Otsuka (1994), who showed that a similar effect can result from E2 core polarization, the case of ${}^8\text{B}$ drew the attention to the possible existence of proton halo.

The firm evidence for the extended spatial distribution of ${}^8\text{B}$ was provided by Schwab et al. (1995) in a measurement of the longitudinal momentum distribution of ${}^7\text{Be}$ following the break-up reaction of ${}^8\text{B}$ beam on different targets. This method is based on the theoretical prediction that the longitudinal momentum distribution (i.e. parallel to the beam direction) resulting from the fragmentation of weakly-bound projectiles is insensitive to details of break-up interactions and provides a reliable probe of the internal momentum wavefunction of the system (Bertulani and McVoy (1992)). For a large spatial extension of the wave function, a narrow momentum distribution is expected. Indeed, using a beam of ${}^8\text{B}$ at about 1.5 GeV/nucleon, Schwab et al. (1995) found a narrow distribution of one-proton-removal product, ${}^7\text{Be}$, with a FWHM of 81 ± 6 MeV/c for carbon, aluminum, and lead targets. This width is smaller by a factor of about 3 from the prediction of the statistical model of fragmentation by Goldhaber (1974) and from the measured values for one-proton removal from other light projectiles.

Another evidence for the unusually large radius of ${}^8\text{B}$ was found soon afterwards. Warner et al. (1995) discovered that the total reaction cross sections, σ_R , for this nucleus on a silicon target was larger than for heavier ${}^{12}\text{C}$ and ${}^{14}\text{N}$ projectiles and notably larger than from conventional calculations.

Two recent results on ${}^8\text{B}$ give a flavour of modern, advanced studies of proton halos. Differential cross sections for elastic proton scattering on ${}^7\text{Be}$ and ${}^8\text{B}$ at an energy 0.7 GeV/nucleon, in inverse kinematics, were measured by Dobrovolsky et al. (2019). Beams of ${}^7\text{Be}$ and ${}^8\text{B}$ impinged on an ionization chamber filled with pure

hydrogen at a pressure of 10 bar, which acted as a target and at the same time as a detector of the recoiling proton (active target). The results were analyzed using Glauber multiple-scattering theory and the matter density distributions were determined. The applied formalism is described in detail by Alkhazov et al. (1978) and the results are shown in Figure 9. By adding one proton to ${}^7\text{Be}$, the tail of the matter distribution changes significantly.

Elastic scattering of ${}^8\text{B}$ on ${}^{64}\text{Zn}$ at much lower energy, close to the Coulomb barrier, was investigated by Sparta et al. (2021) using a post-accelerated ${}^8\text{B}$ beam. The measured data were interpreted with help of the continuum-discretised coupled-channels (CDCC) calculations (Thompson (1988)). The very interesting finding was that in spite the extended matter distribution of ${}^8\text{B}$, its reaction dynamics is very different from that of neutron halo nuclei. In particular, the angular distribution does not show a reduction in the Coulomb-nuclear interference region, like observed for the neutron-halo of ${}^{11}\text{Be}$. This different behaviour is interpreted as due to additional Coulomb halo-core and halo-target interactions. This shows also that the full understanding of the proton-halo dynamics is far from complete even for this best studied case.

${}^{17}\text{F}$

The ground state of ${}^{17}\text{F}$ is $5/2^+$, as expected when a proton is added to the ${}^{16}\text{O}$ core and occupies the $1d_{5/2}$ orbital. The next orbital, $2s_{1/2}$, gives rise to the first excited state $1/2^+$ at 495 keV. Since the proton separation energy from this state is only 105 keV, it is a good candidate for the proton halo. The first hint of that was noticed in the measurement of β decay of ${}^{17}\text{Ne}$ by Borge et al. (1993). They investigated the first-forbidden transition into the first excited state of ${}^{17}\text{F}$ and compared this decay channel with the corresponding mirror transition of ${}^{17}\text{N}$ to ${}^{17}\text{O}$. The difference between the two transitions is quantified by the parameter δ_β :

$$\delta_\beta = \frac{(ft)^+}{(ft)^-} - 1, \quad (7)$$

where $ft^{+/-}$ is the comparative half-life for $\beta^{+/-}$ transitions where one is a mirror of the other. In case of strict mirror symmetry δ_β should be equal to 0, while Borge et al. (1993) found $\delta_\beta = -0.55(9)$. This large asymmetry was explained by the substantial extent of the proton $2s_{1/2}$ orbit and the halo structure of the ${}^{17}\text{F}$ state was postulated. However, as noted by Ozawa et al. (1998), who confirmed the value of δ_β , this finding could also point to an abnormal structure of the ${}^{17}\text{Ne}$ ground state, which is a halo candidate itself, as discussed later.

The confirmation of the halo in ${}^{17}\text{F}$ came from a measurement of the capture cross section for the reaction ${}^{16}\text{O}(p, \gamma){}^{17}\text{F}$ by Morlock et al. (1997). The study was motivated by nuclear astrophysics, as this proton capture reaction is important for the CNO cycle of hydrogen burning in second-generation stars. The authors found that the capture to the first excited $1/2^+$ state in ${}^{17}\text{F}$ strongly increases with the

decreasing energy of protons. This could be explained only by the halo properties of the $1/2^+$ state. A direct-capture model suggested that at the energy of 100 keV (in the center of mass), the main contribution to the capture to the $1/2^+$ state comes from a distance of about 50 fm from the nucleus!

^{26}P and ^{27}P

One of the earliest theoretical predictions of proton-halo candidates was made by Brown and Hansen (1996). Using the shell model they analysed the proton-rich nuclei in the sd shell and suggested three halo candidates: $^{26,27}\text{P}$ and ^{27}S . The latter case will be mentioned a little later, while in this section the isotopes of phosphorus are considered.

The phosphorus isotopes ($Z = 15$) are the lightest nuclei expected to have the last proton in the $2s_{1/2}$ orbital in the ground state. The proton separation energy for ^{26}P and for ^{27}P is 140 keV and 870 keV, respectively. Navin et al. (1998) measured longitudinal momentum distribution of projectile residues after single-nucleon knockout reactions from the beams of phosphorus isotopes. The widths of these distributions were found indeed narrow, as expected for halo structures. Furthermore, the data were consistent with the assumption that the ground states of ^{26}P and ^{27}P are dominated by the s component. The same observation was actually made also for ^{28}P having $S_p = 2052$ keV, which is less favourable for the halo formation.

Fang et al. (2001) produced a number of proton-rich nuclei by a fragmentation of ^{36}Ar beam at the energy of about 70 MeV/nucleon and measured for them the total reaction cross section, σ_R , on a carbon target. The value for ^{27}P was found to be significantly larger than for neighboring nuclei. The density distribution of ^{27}P , determined with help of Glauber-model analysis, revealed the long tail reaching above 12 fm, confirming the proton halo behaviour. No such evidence, however, was found for ^{28}P , and no data for ^{26}P were obtained.

In turn, more light on structure of ^{26}P was shed by a thorough study of its β decay by Pérez-Loureiro et al. (2016). One of the results was the determination of β strength to various final levels in ^{26}Si . In particular, the strength to the first excited 2^+ state was compared with the corresponding mirror transition $^{26}\text{Na}(\beta\gamma)^{26}\text{Mg}$ yielding the large mirror asymmetry $\delta_\beta = 0.51(10)$. The theoretical analysis by ? showed that this finding can be explained by isospin non-conserving forces related to the loosely-bound $2s_{1/2}$ orbit, thus supporting the proton halo hypothesis for ^{26}P .

^{17}Ne

^{17}Ne is the last bound neon isotope, it has the Borromean character (^{16}F is unbound) and has $S_{2p} = 933$ keV – all this makes it a candidate for the two-proton halo. The first firm confirmation of this proposition came from Kanungo et al. (2003). Using the fragmentation of ^{20}Ne primary beam at 135 MeV/nucleon, they produced a beam of ^{17}Ne , which was directed on a 0.5 mm thin beryllium target. The longi-

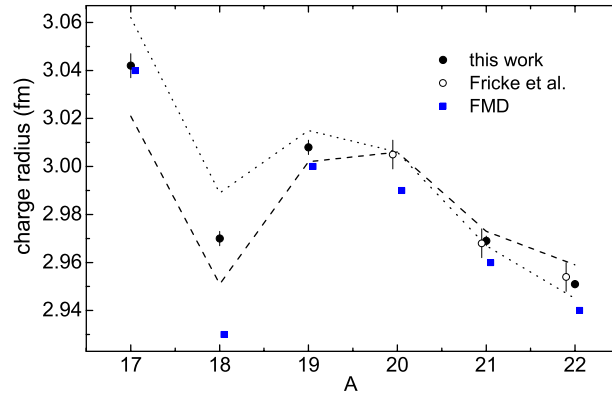


Fig. 10 The rms charge radii for the neon isotopes with mass number A . Error bars indicate the statistical uncertainties. The systematic error limits are represented by the dotted line and the dashed line. From Geithner et al. (2008). Copyright (2008) by the American Physical Society.

tudinal momentum distribution for the two-proton removal was measured, together with the two-proton removal cross section (σ_{-2p}) and the total interaction cross section (σ_I). The width of the momentum distribution was found twice narrower than expected from the Goldhaber (1974) model. In addition, the only consistent description of all measured observables could be obtained assuming that both valence protons occupy the $2s_{1/2}$ orbital. This suggests that between the ^{17}N and its mirror ^{17}Ne the inversion of $1d_{5/2}$ and $2s_{1/2}$ orbitals takes place, which is an example of shell evolution.

Collinear laser spectroscopy is a modern technique for a very precise measurements of nuclear ground-state properties. It is based on the hyperfine interaction between nucleus and atomic electrons. With help of lasers the tiny shifts of electronic states can be measured and from that the nuclear spin, electromagnetic moments, and charge radius can be determined. Using this technique Geithner et al. (2008) made high-precision measurements of charge radii for neon isotopes $^{17-22}\text{Ne}$. The charge radius for ^{17}Ne , 3.042(21) fm, was found to be the largest of all measured. The results were compared with microscopic calculations made in the fermionic molecular dynamics (FMD) framework (Neff and Feldmeier (2008)) which takes into account long-range correlations, like halos or clusters. The FMD approach was found to describe all the data very well, see Figure 10. The conclusion for ^{17}Ne was that its large radius is due to extended proton configuration with an s^2 component of about 40%. In the next isotope, ^{18}Ne , the s^2 admixture is only about 15%, and the radius is smaller.

²²Al and ²⁷S

Recently a detailed β -delayed proton spectroscopy for ²²Si was undertaken by Lee et al. (2020). The properties of β decay branches to low-lying states in ²²Al were measured and compared with the corresponding mirror decay channels of ²²O. For the transition to the first excited 1^+ state a very large asymmetry value, $\delta_\beta = 2.09(96)$ was found. In fact, it is the largest asymmetry ever reported for low-lying states. Since ²²Al has an S_p value close to zero, it could be a signature of the proton halo in this nucleus.

A similar observation, first indicated by Janiak et al. (2017) and later confirmed with higher accuracy by Sun et al. (2019), was made for the β decay of ²⁷S. The transitions to the first excited states $3/2^+$ and $5/2^+$ in ²⁷P, compared to data for the mirror decay channels in the decay of ²⁷Na, revealed strong asymmetry with δ_β equal to 0.38(26) and 0.48(18), respectively. This could point to the two-proton halo in ²⁷S: the two last protons in this nucleus should occupy the $2s_{1/2}$ orbital, the separation energy is $S_{2p} = 728(78)$ keV, and it was among the first proton-halo candidates predicted by Brown and Hansen (1996).

The mirror asymmetry in β decay may result from abnormal structure of the initial and/or the final nucleus. The β daughter of ²⁷S is ²⁷P, which is already an established proton-halo nucleus. It is not excluded that in ²²Si, which is at the proton dripline, the valence protons have a substantial $2s_{1/2}$ component. On the other hand, the mirror asymmetries reported for β decays of ²²Si and ²⁷S were calculated using the available data for the mirror nuclei, ²²O and ²⁷Na. As noted by Guadilla et al. (2021) decay schemes for the latter seem to be incomplete and must be remeasured with higher accuracy before firm conclusions concerning mirror asymmetry are drawn.

It may turn out that all four nuclei, ²⁷S, ²⁷P, ²²Si, and ²²Al exhibit features of proton halo, but to assess that, certainly more experimental and theoretical studies are needed. Actually, more investigations are required for all cases discussed in this section to gain the complete understanding of the proton-halo phenomenon, and for sure this will remain an important research topic in the near future.

7 Proton dripline nuclei and nucleosynthesis

Nuclei in the proximity of the proton dripline play an important role also in energy generation in high-temperature hydrogen burning (X-ray bursts, novae) and in the nucleosynthesis of the heavier nuclei via the so-called rapid proton-capture (rp-) process. The latter consists in a sequence of proton captures and β decays responsible for the burning of hydrogen into heavier elements under extreme conditions of temperature and density. This network of nuclear reactions and decays proceeds close to the proton dripline and $N \approx Z$ all the way to the ¹⁰⁰Sn region, see the review by Schatz et al. (1998) for details. A limiting parameter for the reaction path followed by the rp-process is given by the proton dripline, since proton capture is

hindered by the negative separation energy and β decay therefore prevails. Such limit could be overcome by two-proton capture on the last proton-bound isotone, but such process is not going to be dominant. If the reaction flow reaches a proton-unbound nucleus or photo-disintegration reaction rates for an isotope in the flow are inhibiting further proton-capture reactions, the reaction flow reaches a “bottleneck” and has to wait for the relatively slow β decay to proceed further. The “bottleneck” nucleus is called a waiting point.

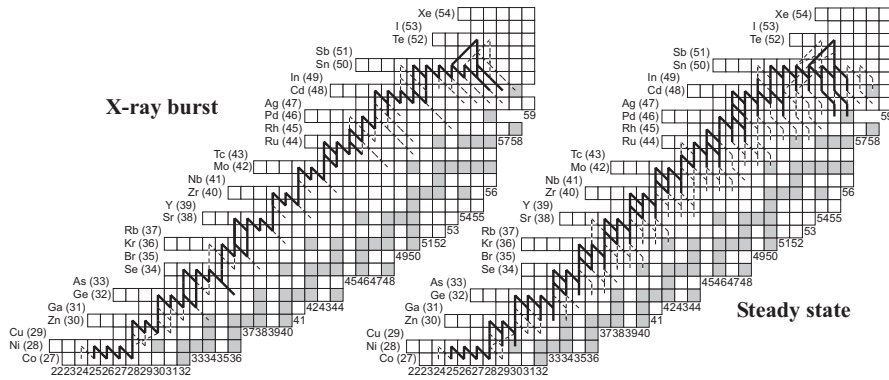


Fig. 11 Time-integrated reaction flow calculated for an X-ray burst and a steady-state burning. Only the portion of the flow progressing beyond zinc and germanium is shown. Figure from the work by Schatz et al. (2001). Copyright (2001) by the American Physical Society.

The flow, abundance patterns and energy output predicted by modelling of the rp-process are extremely sensitive to the properties of the nuclei involved in the process. It was shown by Schatz et al. (1998) that the nuclear structure parameters that have the most impact on the modelling are nuclear masses, since the main contribution to the shape of the rp-process path is given by proton separation energies and Q -values. Also very important are β -decay half-lives and branching ratios for delayed proton emission, which control the time structure and final abundances, in particular those of the waiting points. Two-proton capture becomes important in a high-density environment, since it can speed up the flow towards heavier nuclei. It is therefore vital to determine the properties of the nuclei involved in the rp-process, and to validate nuclear models that provide such properties for those isotopes still not accessible in the laboratory. Excited states in waiting point nuclei can also play a role in the rp-process flow, in particular low-lying ones, which are populated at higher temperatures. At temperatures of the order of 1-2 GK the contribution to the flow from the decay of excited states cannot be ignored and may become of the same order of the contribution of the ground state (Sarriguren (2011)).

A notable example of the impact of nuclear masses on the rp-process flow is illustrated by calculations that predicted that, once the process reaches the tin isotopes with $A = 99-101$, it follows the isotopic chain towards less exotic nuclei and then gets “trapped” into a cycle around tin-antimony-tellurium isotopes (Schatz et al.

(2001)), see Figure 11. The cycling is due to the fact that the tellurium isotopes involved are α unbound and decay back to tin. Whether the cycling around SnSbTe isotopes occurs or not, is entirely dependent on the nuclear physics input to the calculations (binding energies, half-lives, branching ratios). The occurrence or not of the cycle has important consequences for energy/light production and composition of the ashes of the process. In fact, such a cycle, which happens late in the process, produces helium, providing additional α particles that fuel reactions at later times. Intriguing is the impact of the proton separation energy in the most neutron-deficient antimony isotopes on the termination of the rp-process. In fact, the precise determination of the proton-separation energy in ^{105}Sb and ^{106}Sb led to a new scenario for the rp-process path beyond ^{100}Sn (Elomaa et al. (2009); Mazzocchi et al. (2007)), excluding almost entirely the cycling around SnSbTe isotopes by confining its contribution to a level of 3%. The absence of strong cycling has the consequence of reducing production of helium at late times.

Nuclear properties of exotic nuclei taking part into the rp-process, like proton and γ widths (Γ_p and Γ_γ) for excited states involved in the (p, γ) and (γ, p) reaction along the path, are often determined by means of indirect methods, given that such nuclei are not easily accessible for direct reaction studies. A few examples of such approaches can be found in the works by Langer et al. (2014); Kennington et al. (2021); Koldste et al. (2013)

8 Conclusions

In this chapter an overview on the proton rich edge of the chart of nuclei was presented and the main features and phenomena which characterise these very proton-rich nuclei were introduced. Of course, not all interesting results and research ideas pertaining to the proton dripline region could be mentioned, and illustrative examples which are most enticing in the authors opinion were selected. The goal was to attract the reader to this domain of nuclear physics, and to suggest links for further learning, rather than to provide an exhaustive report.

One important aspect of proton dripline physics, is how much different research approaches are intertwined. The same nucleus attracts attention for various reasons, and different research methods, focused on different facets of its structure, only in combination, yield the complete picture. For example the $1/2^+$ state in ^{17}F is the subject to the Thomas-Ehrman shift, which leads to the proton halo feature, which in turn affects the reaction rates of astrophysical importance. The ^{100}Sn and its region is a “holy grail” for the shell-model, a potential reference point for α spectroscopy, and a key point in the rp-process. Studies of isospin symmetry bring information on nuclear forces but also deliver hints of anomalous nuclear behaviour. Complementarity of methods is the way to follow in this field.

Finally, a few remarks concerning the future prospects of this field are worth noting. The exploration of proton-rich nuclei continues and the territory reached by experiment, marked in Figures 2 and 3, will soon expand. The new Facility for

Rare Isotope Beams (FRIB, see Sherrill (2018)) is just about to start operations. According to estimates made by Neufcourt et al. (2020a) the FRIB may shift the line of accessible isotopes by up to 5 neutrons away from the current limit. In total, about 120 new isotopes, between zirconium and uranium, are expected to be delivered for studies.

When looking at the Figures 2 and 3 one question which suggests itself is how high in Z number the $2p$ radioactivity can occur and to how low Z values the observable p emission will range. The progress in both these lines of study requires increased production yields of nuclei beyond the dripline. The search for light p -emitters will depend, in addition, on advances in fast techniques of separation and detection, and on fast data acquisition methods which rely to increasing extend on digital signal processing.

A more quantitative answer to the range of ground-state $2p$ emission was attempted by Olsen et al. (2013b,a). Using advanced predictions of nuclear separation energies Erler et al. (2012), and simplified models of $2p$ and α decays, they inquired for which nuclei the $2p$ half-life may be longer than 100 ns, to be detectable using the in-flight technique, and short enough to compete with other decay modes (β^+ , α). The main conclusion was that conditions for $2p$ radioactivity can appear for all even- Z elements between argon and tellurium. Between xenon and lead, however, a different picture emerged. Due to high Coulomb barrier, for the simultaneous emission of two protons to be the dominant decay, one has to go so far beyond the dripline, that a single proton becomes unbound. In consequence, the two protons are emitted, but in sequence, one after the other (pp). Above lead, α decay was found to dominate totally. This general picture was confirmed by a recent calculation based on the Bayesian Model Averaging method by Neufcourt et al. (2020a).

This kind of predictions are very approximate, nevertheless it seems certain that when going along the proton dripline towards lead, the region between the dripline and the line of dominating proton emission, becomes wider and wider. A spacious proton-rich *terra incognita* appears which could be addressed with classical nuclear spectroscopy. To what extent it will be possible to explore this territory, shall be seen when the new generation of radioactive beam facilities, like FRIB at MSU, FAIR at GSI, SPIRAL2 at GANIL, RAON in Korea, will come into operation.

References

- G.D. Alkhozov, S.L. Belostotsky, A.A. Vorobyov, Scattering of 1 GeV protons on nuclei. *Physics Reports* **42**(2), 89–144 (1978). [https://doi.org/10.1016/0370-1573\(78\)90083-2](https://doi.org/10.1016/0370-1573(78)90083-2). <https://www.sciencedirect.com/science/article/pii/0370157378900832>
- P. Ascher, L. Audirac, N. Adimi, B. Blank, C. Borcea, B.A. Brown, I. Companis, F. Delalée, C.E. Demonchy, F. de Oliveira Santos, J. Giovinazzo, S. Grévy, L.V. Grigorenko, T. Kurtukian-Nieto, S. Leblanc, J.-L. Pedroza, L. Perrot, J. Pibernat, L. Serani, P.C. Srivastava, J.-C. Thomas, Direct observation of two protons in the decay of ^{54}Zn . *Phys. Rev. Lett.* **107**, 102502 (2011). <https://doi.org/10.1103/PhysRevLett.107.102502>. <https://link.aps.org/doi/10.1103/PhysRevLett.107.102502>

- K. Auranen, D. Seweryniak, M. Albers, A.D. Ayangeakaa, S. Bottoni, M.P. Carpenter, C.J. Chiara, P. Copp, H.M. David, D.T. Doherty, J. Harker, C.R. Hoffman, R.V.F. Janssens, T.L. Khoo, S.A. Kuvin, T. Lauritsen, G. Lotay, A.M. Rogers, J. Sethi, C. Scholey, R. Talwar, W.B. Walters, P.J. Woods, S. Zhu, Superallowed α decay to doubly magic ^{100}Sn . *Phys. Rev. Lett.* **121**, 182501 (2018). <https://doi.org/10.1103/PhysRevLett.121.182501>
<https://link.aps.org/doi/10.1103/PhysRevLett.121.182501>
- J. Äystö, Development and applications of the igisol technique. *Nuclear Physics A* **693**(1-2), 477–494 (2001). [https://doi.org/DOI:10.1016/S0375-9474\(01\)00923-X](https://doi.org/DOI:10.1016/S0375-9474(01)00923-X)
- R. Barton, R. McPherson, R.E. Bell, W.R. Frisken, W.T. Link, R.B. Moore, Observation of delayed proton radioactivity. *Canadian Journal of Physics* **41**, 2007–2025 (1963). <https://doi.org/10.1139/p63-201>
- J.C. Batchelder, Recommended values for β^+ -delayed proton and α emission. *Atomic Data and Nuclear Data Tables* **132**, 101323 (2020). <https://doi.org/10.1016/j.adt.2019.101323>
<https://www.sciencedirect.com/science/article/pii/S0092640X19300865>
- D. Bazin, R. Del Moral, J.P. Dufour, A. Fleury, F. Hubert, M.S. Pravikoff, R. Anne, P. Bricault, C. Détraz, M. Lewitowicz, Y. Zheng, D. Guillemaud-Mueller, J.C. Jacmart, A.C. Mueller, F. Pougheon, A. Richard, Decay modes of ^{31}Ar and first observation of β -delayed three-proton radioactivity. *Phys. Rev. C* **45**, 69–79 (1992). <https://doi.org/10.1103/PhysRevC.45.69>
<https://link.aps.org/doi/10.1103/PhysRevC.45.69>
- M.A. Bentley, S.M. Lenzi, Coulomb energy differences between high-spin states in isobaric multiplets. *Progress in Particle and Nuclear Physics* **59**(2), 497–561 (2007). <https://doi.org/10.1016/j.pnnp.2006.10.001>
<https://www.sciencedirect.com/science/article/pii/S0146641006000743>
- C.A. Bertulani, K.W. McVoy, Momentum distributions in reactions with radioactive beams. *Phys. Rev. C* **46**, 2638–2641 (1992). <https://doi.org/10.1103/PhysRevC.46.2638>
<https://link.aps.org/doi/10.1103/PhysRevC.46.2638>
- B. Blank, M.J.G. Borge, Nuclear structure at the proton drip line: Advances with nuclear decay studies. *Progress in Particle and Nuclear Physics* **60**(2), 403–483 (2008). <https://doi.org/10.1016/j.pnnp.2007.12.001>
<https://www.sciencedirect.com/science/article/pii/S0146641007000956>
- B. Blank, A. Bey, G. Cachel, C. Dossat, A. Fleury, J. Giovinazzo, I. Matea, N. Adimi, F. De Oliveira, I. Stefan, G. Georgiev, S. Grévy, J.C. Thomas, C. Borcea, D. Cortina, M. Caamano, M. Stanoiu, F. Aksouh, B.A. Brown, F.C. Barker, W.A. Richter, First observation of ^{54}Zn and its decay by two-proton emission. *Phys. Rev. Lett.* **94**, 232501 (2005). <https://doi.org/10.1103/PhysRevLett.94.232501>
<https://link.aps.org/doi/10.1103/PhysRevLett.94.232501>
- B. Blank, L. Hay, J. Huikari, S. Leblanc, S. List, J.-L. Pedroza, P. Ascher, L. Audirac, C. Borcea, G. Cachel, F. Delalee, C.E. Demonchy, C. Dossat, J. Giovinazzo, P. Hellmuth, C. Marchand, I. Matea, R. de Oliveira, J. Pibernat, A. Rebi, L. Serani, J.C. Thomas, A time projection chamber for the three-dimensional reconstruction of two-proton radioactivity events. *Nuclear Instruments and Methods in Physics Research Section A: Accelerators, Spectrometers, Detectors and Associated Equipment* **613**(1), 65–78 (2010). <https://doi.org/10.1016/j.nima.2009.10.140>
<https://www.sciencedirect.com/science/article/pii/S0168900209020920>
- B. Blank, M. Płoszajczak, Two-proton radioactivity. *Reports on Progress in Physics* **71**(4), 046301 (2008). <https://doi.org/10.1088/0034-4885/71/4/046301>
<https://doi.org/10.1088/0034-4885/71/4/046301>
- O.V. Bochkarev, A.A. Korshennikov, E.A. Kuz'min, I.G. Mukha, A.A. Ogloblin, L.V. Chulkov, G.B. Yan'kov, Two-proton decay of ^6Be . *JETP Lett.* **40**, 969–972 (1984). *Pis'ma Zh. Eksp. Teor. Fiz.* **40** (1984) 204–207
- R. Bonetti, A. Guglielmetti, Cluster radioactivity: an overview after twenty years. *Romanian Reports in Physics* **59**, 301–310 (2007)
- M.J.G. Borge, J. Deding, P.G. Hansen, B. Jonson, G. Martínez Pinedo, P. Moller, G. Nyman, A. Poves, A. Richter, K. Riisager, O. Tengblad, Beta-decay to the proton halo state in

- 17F. *Physics Letters B* **317**(1), 25–30 (1993). [https://doi.org/10.1016/0370-2693\(93\)91564-4](https://doi.org/10.1016/0370-2693(93)91564-4). <https://www.sciencedirect.com/science/article/pii/0370269393915644>
- B.A. Brown, P.G. Hansen, Proton halos in the $1s_{0d}$ shell. *Physics Letters B* **381**(4), 391–396 (1996). [https://doi.org/10.1016/0370-2693\(96\)00634-X](https://doi.org/10.1016/0370-2693(96)00634-X). <https://www.sciencedirect.com/science/article/pii/037026939600634X>
- M.D. Cable, J. Honkanen, R.F. Parry, S.H. Zhou, Z.Y. Zhou, J. Cerny, Discovery of beta-delayed two-proton radioactivity: ^{22}Al . *Phys. Rev. Lett.* **50**, 404–406 (1983). <https://doi.org/10.1103/PhysRevLett.50.404>. <https://link.aps.org/doi/10.1103/PhysRevLett.50.404>
- L. Capponi, J.F. Smith, P. Ruotsalainen, C. Scholey, P. Rakhila, K. Auranen, L. Bianco, A.J. Boston, H.C. Boston, D.M. Cullen, X. Derkx, M.C. Drummond, T. Grahn, P.T. Greenlees, L. Grocutt, B. Hadinia, U. Jakobsson, D.T. Joss, R. Julin, S. Juutinen, M. Labiche, M. Leino, K.G. Leach, C. McPeake, K.F. Mulholland, P. Nieminen, D. O'Donnell, E.S. Paul, P. Peura, M. Sandzelius, J. Sarén, B. Saygi, J. Sorri, S. Stolze, A. Thornthwaite, M.J. Taylor, J. Uusitalo, Direct observation of the $^{114}\text{Ba} \rightarrow ^{110}\text{Xe} \rightarrow ^{106}\text{Te} \rightarrow ^{102}\text{Sn}$ triple α -decay chain using position and time correlations. *Phys. Rev. C* **94**, 024314 (2016). <https://doi.org/10.1103/PhysRevC.94.024314>. <https://link.aps.org/doi/10.1103/PhysRevC.94.024314>
- R.J. Charity, J.M. Elson, J. Manfredi, R. Shane, L.G. Sobotka, B.A. Brown, Z. Chajecski, D. Coupland, H. Iwasaki, M. Kilburn, J. Lee, W.G. Lynch, A. Sanetullaev, M.B. Tsang, J. Winkelbauer, M. Youngs, S.T. Marley, D.V. Shetty, A.H. Wuosmaa, T.K. Ghosh, M.E. Howard, Investigations of three-, four-, and five-particle decay channels of levels in light nuclei created using a ^9C beam. *Phys. Rev. C* **84**, 014320 (2011). <https://doi.org/10.1103/PhysRevC.84.014320>. <https://link.aps.org/doi/10.1103/PhysRevC.84.014320>
- J.C. Chow, J.D. King, N.P.T. Bateman, R.N. Boyd, L. Buchmann, J.M. D'Auria, T. Davinson, M. Dombisky, E. Gete, U. Giesen, C. Iliadis, K.P. Jackson, A.C. Morton, J. Powell, A. Shotter, β -delayed particle decay of ^{17}Ne into $p + \alpha + ^{12}\text{C}$ through the isobaric analog state in ^{17}F . *Phys. Rev. C* **66**, 064316 (2002). <https://doi.org/10.1103/PhysRevC.66.064316>. <https://link.aps.org/doi/10.1103/PhysRevC.66.064316>
- R.M. Clark, A.O. Macchiavelli, H.L. Crawford, P. Fallon, D. Rudolph, A. Sâmark-Roth, C.M. Campbell, M. Cromaz, C. Morse, C. Santamaria, Enhancement of α -particle formation near ^{100}Sn . *Phys. Rev. C* **101**, 034313 (2020). <https://doi.org/10.1103/PhysRevC.101.034313>. <https://link.aps.org/doi/10.1103/PhysRevC.101.034313>
- I.G. Darby, R.K. Grzywacz, J.C. Batchelder, C.R. Bingham, L. Cartegni, C.J. Gross, M. Hjorth-Jensen, D.T. Joss, S.N. Liddick, W. Nazarewicz, S. Padgett, R.D. Page, T. Papenbrock, M.M. Rajabali, J. Rotureau, K.P. Rykaczewski, Orbital dependent nucleonic pairing in the lightest known isotopes of tin. *Phys. Rev. Lett.* **105**(16), 162502 (2010). <https://doi.org/10.1103/PhysRevLett.105.162502>
- C.N. Davids, B.B. Back, K. Bindra, D.J. Henderson, W. Kutschera, T. Lauritsen, Y. Nagame, P. Sugathan, A.V. Ramayya, W.B. Walters, Startup of the fragment mass analyzer at atlas. *Nuclear Instruments and Methods in Physics Research Section B: Beam Interactions with Materials and Atoms* **70**(1), 358–365 (1992). [https://doi.org/10.1016/0168-583X\(92\)95951-M](https://doi.org/10.1016/0168-583X(92)95951-M). <https://www.sciencedirect.com/science/article/pii/0168583X9295951M>
- D.S. Delion, A. Dumitrescu, Universal proton emission systematics. *Phys. Rev. C* **103**, 054325 (2021). <https://doi.org/10.1103/PhysRevC.103.054325>. <https://link.aps.org/doi/10.1103/PhysRevC.103.054325>
- A.V. Dobrovolsky, G.A. Korolev, A.G. Inglessi, G.D. Alkhazov, G. Colo, I. Dillmann, P. Egelhof, A. Estradé, F. Farinon, H. Geissel, S. Ilieva, Y. Ke, A.V. Khanzadeev, O.A. Kiselev, J. Kurcewicz, X.C. Le, Y.A. Litvinov, G.E. Petrov, A. Prochazka, C. Scheidenberger, L.O. Sergeev, H. Simon, M. Takechi, S. Tang, V. Volkov, A.A. Vorobyov, H. Weick, V.I. Yatsoura, Nuclear-matter distribution in the proton-rich nuclei 7Be and 8B from intermediate energy proton elastic scattering in inverse kinematics. *Nuclear Physics A* **989**, 40–58 (2019). <https://doi.org/10.1016/j.nuclphysa.2019.05.012>. <https://www.sciencedirect.com/science/article/pii/S0375947419301186>

- P. Doornenbal, P. Reiter, H. Grawe, T. Otsuka, A. Al-Khatib, A. Banu, T. Beck, F. Becker, P. Bednarczyk, G. Benzoni, A. Bracco, A. Bürger, L. Caceres, F. Camera, S. Chmel, F.C.L. Crespi, H. Geissel, J. Gerl, M. Görska, J. Grebosz, H. Hübel, M. Kavatsyuk, O. Kavatsyuk, M. Kmiecik, I. Kojouharov, N. Kurz, R. Lozeva, A. Maj, S. Mandal, W. Meczynski, B. Million, Z. Podolyák, A. Richard, N. Saito, T. Saito, H. Schaffner, M. Seidlitz, T. Striepling, Y. Utsuno, J. Walker, N. Warr, H. Weick, O. Wieland, M. Winkler, H.J. Wollersheim, The $T=2$ mirrors ^{36}Ca and ^{36}S : A test for isospin symmetry of shell gaps at the driplines. *Physics Letters B* **647**(4), 237–242 (2007). <https://doi.org/10.1016/j.physletb.2007.02.001>. <https://www.sciencedirect.com/science/article/pii/S0370269307001499>
- J.B. Ehrman, On the displacement of corresponding energy levels of ^{13}C and ^{13}N . *Phys. Rev.* **81**, 412–416 (1951). <https://doi.org/10.1103/PhysRev.81.412>. <https://link.aps.org/doi/10.1103/PhysRev.81.412>
- V.-V. Elomaa, G.K. Vorobjev, A. Kankainen, L. Batist, S. Eliseev, T. Eronen, J. Hakala, A. Jokinen, I.D. Moore, Y.N. Novikov, H. Penttilä, A. Popov, S. Rahaman, J. Rissanen, A. Saastamoinen, H. Schatz, D.M. Seliverstov, C. Weber, J. Äystö, Quenching of the SnSbTe cycle in the rp process. *Phys. Rev. Lett.* **102**, 252501 (2009). <https://doi.org/10.1103/PhysRevLett.102.252501>. <https://link.aps.org/doi/10.1103/PhysRevLett.102.252501>
- ENSDF database, 2022. Accessed 22 February 2022. <https://www.nndc.bnl.gov/ensdf/>
- J. Erler, N. Birge, M. Kortelainen, W. Nazarewicz, E. Olsen, A.M. Perhac, M. Stoitsov, The limits of the nuclear landscape. *Nature* **486**(7404), 509–512 (2012). <https://doi.org/10.1038/nature11188>. <https://doi.org/10.1038/nature11188>
- T. Faestermann, M. Görska, H. Grawe, The structure of ^{100}Sn and neighbouring nuclei. *Progress in Particle and Nuclear Physics* **69**, 85–130 (2013). <https://doi.org/10.1016/j.pnpnp.2012.10.002>. <https://www.sciencedirect.com/science/article/pii/S0146641012001172>
- D.Q. Fang, W.Q. Shen, J. Feng, X.Z. Cai, H.Y. Zhang, Y.G. Ma, C. Zhong, Z.Y. Zhu, W.Z. Jiang, W.L. Zhan, Z.Y. Guo, G.Q. Xiao, J.S. Wang, J.Q. Wang, J.X. Li, M. Wang, J.F. Wang, Z.J. Ning, Q.J. Wang, Z.Q. Chen, Evidence for a proton halo in ^{27}P through measurements of reaction cross-sections at intermediate energies. *The European Physical Journal A - Hadrons and Nuclei* **12**(3), 335–339 (2001). <https://doi.org/10.1007/s100500170011>. <https://doi.org/10.1007/s100500170011>
- V.N. Fedosseev, L.-E. Berg, D.V. Fedorov, D. Fink, O.J. Launila, R. Losito, B.A. Marsh, R.E. Rossel, S. Rothe, M.D. Seliverstov, A.M. Sjodin, K.D.A. Wendt, Upgrade of the resonance ionization laser ion source at isolde on-line isotope separation facility: New lasers and new ion beams. *Review of Scientific Instruments* **83**(2), 02–903 (2012). <https://doi.org/10.1063/1.3662206>. <https://doi.org/10.1063/1.3662206>
- H.O.U. Fynbo, L. Axelsson, J. Äystö, M.J.G. Borge, L.M. Fraile, A. Honkanen, P. Hornshøj, Y. Jading, A. Jokinen, B. Jonson, I. Martel, I. Mukha, T. Nilsson, G. Nyman, M. Oinonen, K. Riisager, T. Siiskonen, M.H. Smedberg, O. Tengblad, F. Wenander, ^{31}Ar examined: New limit on the β -delayed three-proton branch. *Phys. Rev. C* **59**, 2275–2277 (1999). <https://doi.org/10.1103/PhysRevC.59.2275>. <https://link.aps.org/doi/10.1103/PhysRevC.59.2275>
- H.O.U. Fynbo, M.J.G. Borge, L. Axelsson, J. Äystö, U.C. Bergmann, L.M. Fraile, A. Honkanen, P. Hornshøj, Y. Jading, A. Jokinen, B. Jonson, I. Martel, I. Mukha, T. Nilsson, G. Nyman, M. Oinonen, I. Piqueras, K. Riisager, T. Siiskonen, M.H. Smedberg, O. Tengblad, J. Thaysen, F. Wenander, The β_{2p} decay mechanism of ^{31}Ar . *Nuclear Physics A* **677**(1), 38–60 (2000). [https://doi.org/10.1016/S0375-9474\(00\)00248-7](https://doi.org/10.1016/S0375-9474(00)00248-7). <https://www.sciencedirect.com/science/article/pii/S0375947400002487>
- J.-J. Gaimard, K.-H. Schmidt, A reexamination of the abrasion-ablation model for the description of the nuclear fragmentation reaction. *Nuclear Physics A* **531**(3-4), 709–745 (1991). [https://doi.org/DOI:10.1016/0375-9474\(91\)90748-U](https://doi.org/DOI:10.1016/0375-9474(91)90748-U)
- G. Gamow, Fine structure of α -rays. *Nature* **126**(3176), 397–397 (1930). <https://doi.org/10.1038/126397a0>. <https://doi.org/10.1038/126397a0>

- D.F. Geesaman, R.L. McGrath, P.M.S. Lesser, P.P. Urone, B. VerWest, Particle decay of ${}^6\text{Be}$. *Phys. Rev. C* **15**, 1835–1838 (1977). <https://doi.org/10.1103/PhysRevC.15.1835>. <https://link.aps.org/doi/10.1103/PhysRevC.15.1835>
- H. Geissel, P. Armbruster, K.H. Behr, A. Brünle, K. Burkard, M. Chen, H. Folger, B. Franczak, H. Keller, O. Klepper, B. Langenbeck, F. Nickel, E. Pfeng, M. Pfützner, E. Roeckl, K. Rykaczewski, I. Schall, D. Schardt, C. Scheidenberger, K.-H. Schmidt, A. Schröter, T. Schwab, K. Sümmerer, M. Weber, G. Münzenberg, T. Brohm, H.-G. Clerc, M. Fauerbach, J.-J. Gaimard, A. Grewe, E. Hanelt, B. Knödler, M. Steiner, B. Voss, J. Weckenmann, C. Ziegler, A. Magel, H. Wollnik, J.P. Dufour, Y. Fujita, D.J. Vieira, B. Sherrill, The GSI projectile fragment separator (FRS): a versatile magnetic system for relativistic heavy ions. *Nuclear Instruments and Methods in Physics Research Section B: Beam Interactions with Materials and Atoms* **70**(1), 286–297 (1992). [https://doi.org/10.1016/0168-583X\(92\)95944-M](https://doi.org/10.1016/0168-583X(92)95944-M). <https://www.sciencedirect.com/science/article/pii/0168583X9295944M>
- W. Geithner, T. Neff, G. Audi, K. Blaum, P. Delahaye, H. Feldmeier, S. George, C. Guénaut, F. Herfurth, A. Herlert, S. Kappertz, M. Keim, A. Kellerbauer, H.-J. Kluge, M. Kowalska, P. Lievens, D. Lunney, K. Marinova, R. Neugart, L. Schweikhard, S. Wilbert, C. Yazidjian, Masses and charge radii of ${}^{17-22}\text{Ne}$ and the two-proton-halo candidate ${}^{17}\text{Ne}$. *Phys. Rev. Lett.* **101**, 252502 (2008). <https://doi.org/10.1103/PhysRevLett.101.252502>. <https://link.aps.org/doi/10.1103/PhysRevLett.101.252502>
- E. Gete, L. Buchmann, R.E. Azuma, D. Anthony, N. Bateman, J.C. Chow, J.M. D’Auria, M. Domb-sky, U. Giesen, C. Iliadis, K.P. Jackson, J.D. King, D.F. Measday, A.C. Morton, β -delayed particle decay of ${}^9\text{C}$ and the $A = 9, T = 1/2$ nuclear system: Experiment, data, and phenomenological analysis. *Phys. Rev. C* **61**, 064310 (2000). <https://doi.org/10.1103/PhysRevC.61.064310>. <https://link.aps.org/doi/10.1103/PhysRevC.61.064310>
- J. Giovinazzo, B. Blank, M. Chartier, S. Czajkowski, A. Fleury, M.J. Lopez Jimenez, M.S. Pravikoff, J.-C. Thomas, F. de Oliveira Santos, M. Lewitowicz, V. Maslov, M. Stanoiu, R. Grzywacz, M. Pfützner, C. Borcea, B.A. Brown, Two-proton radioactivity of ${}^{45}\text{Fe}$. *Phys. Rev. Lett.* **89**, 102501 (2002). <https://doi.org/10.1103/PhysRevLett.89.102501>. <https://link.aps.org/doi/10.1103/PhysRevLett.89.102501>
- J. Giovinazzo, B. Blank, C. Borcea, G. Cachel, J.-C. Dalouzy, C.E. Demonchy, F. de Oliveira Santos, C. Dossat, S. Grévy, L. Hay, J. Huikari, S. Leblanc, I. Matea, J.-L. Pedroza, L. Perrot, J. Pibernat, L. Serani, C. Stodel, J.-C. Thomas, First direct observation of two protons in the decay of ${}^{45}\text{Fe}$ with a time-projection chamber. *Phys. Rev. Lett.* **99**, 102501 (2007). <https://doi.org/10.1103/PhysRevLett.99.102501>. <https://link.aps.org/doi/10.1103/PhysRevLett.99.102501>
- T. Goigoux, P. Ascher, B. Blank, M. Gerbaux, J. Giovinazzo, S. Grévy, T. Kurtukian Nieto, C. Magron, P. Doornenbal, G.G. Kiss, S. Nishimura, P.-A. Söderström, V.H. Phong, J. Wu, D.S. Ahn, N. Fukuda, N. Inabe, T. Kubo, S. Kubono, H. Sakurai, Y. Shimizu, T. Sumikama, H. Suzuki, H. Takeda, J. Agramunt, A. Algora, V. Guadilla, A. Montaner-Piza, A.I. Morales, S.E.A. Orrigo, B. Rubio, Y. Fujita, M. Tanaka, W. Gelletly, P. Aguilera, F. Molina, F. Diel, D. Lubos, G. de Angelis, D. Napoli, C. Borcea, A. Boso, R.B. Cakirli, E. Ganioglu, J. Chiba, D. Nishimura, H. Oikawa, Y. Takei, S. Yagi, K. Wimmer, G. de France, S. Go, B.A. Brown, Two-proton radioactivity of ${}^{67}\text{Kr}$. *Phys. Rev. Lett.* **117**, 162501 (2016). <https://doi.org/10.1103/PhysRevLett.117.162501>. <https://link.aps.org/doi/10.1103/PhysRevLett.117.162501>
- V.I. Goldansky, On neutron-deficient isotopes of light nuclei and the phenomena of proton and two-proton radioactivity. *Nuclear Physics* **19**, 482–495 (1960). [https://doi.org/10.1016/0029-5582\(60\)90258-3](https://doi.org/10.1016/0029-5582(60)90258-3). <https://www.sciencedirect.com/science/article/pii/0029558260902583>
- A.S. Goldhaber, Statistical models of fragmentation processes. *Physics Letters B* **53**(4), 306–308 (1974). [https://doi.org/10.1016/0370-2693\(74\)90388-8](https://doi.org/10.1016/0370-2693(74)90388-8). <https://www.sciencedirect.com/science/article/pii/0370269374903888>
- L.V. Grigorenko, M.V. Zhukov, Two-proton radioactivity and three-body decay. ii. Exploratory studies of lifetimes and correlations. *Phys.*

- Rev. C **68**, 054005 (2003). <https://doi.org/10.1103/PhysRevC.68.054005>
<https://link.aps.org/doi/10.1103/PhysRevC.68.054005>
- V. Guadilla, M. Pfützner, J. Agramunt, A. Algora, A. Andreyev, G. de Angelis, A. Beloeuvre, J. Benito, M.J.G. Borge, J.A. Briz, T.D. Bucher, M. Estienne, M. Fallot, A. Fijałkowska, L.M. Fraile, E. Ganioglu, W. Gelletly, L. Giot, A. Illana, Z. Janas, M. Karny, A. Korgul, R. Lica, C. Mazzocchi, F. Molina, A.I. Morales, B. Nacher E. and Olaizola, N. Orce, S.E.A. Origo, J. Pakarinen, A. Perea, M. Piersa, Z. Podolyak, A. Porta, B. Rubio, J.L. Tain, M.O.T. M. Stryczyk, Beta-decay spectroscopy of ^{27}Na and ^{22}O for isospin asymmetry studies in the sd shell, 2021. Report CERN-INTC-2021-004 ; INTC-P-590
- A. Guglielmetti, B. Blank, R. Bonetti, Z. Janas, H. Keller, R. Kirchner, O. Klepper, A. Piechaczek, A. Plochocki, G. Poli, P.B. Price, E. Roeckl, K. Schmidt, J. Szerypo, A.J. Westphal, Production of ^{114}Ba in $^{58}\text{Ni} + ^{58}\text{Ni}$ reactions and detection of its cluster radioactivity. Nuclear Physics A **583**, 867–870 (1995). Nucleus-Nucleus Collisions. [https://doi.org/10.1016/0375-9474\(94\)00776-J](https://doi.org/10.1016/0375-9474(94)00776-J). <https://www.sciencedirect.com/science/article/pii/037594749400776J>
- A. Guglielmetti, R. Bonetti, G. Poli, R. Collatz, Z. Hu, R. Kirchner, E. Roeckl, N. Gunn, P.B. Price, B.A. Weaver, A. Westphal, J. Szerypo, Nonobservation of ^{12}C cluster decay of ^{114}Ba . Phys. Rev. C **56**, 2912–2916 (1997). <https://doi.org/10.1103/PhysRevC.56.R2912>
<https://link.aps.org/doi/10.1103/PhysRevC.56.R2912>
- J.C. Hardy, I.S. Towner, Superaligned $0^+ \rightarrow 0^+$ nuclear β decays: 2020 critical survey, with implications for V_{ud} and ckm unitarity. Phys. Rev. C **102**, 045501 (2020). <https://doi.org/10.1103/PhysRevC.102.045501>
<https://link.aps.org/doi/10.1103/PhysRevC.102.045501>
- HIE-ISOLDE <https://hie-isolde-project.web.cern.ch/hie-isolde-project>
- C.B. Hinke, M. Bohmer, P. Boutachkov, T. Faestermann, H. Geissel, J. Gerl, R. Gernhauser, M. Gorska, A. Gottardo, H. Grawe, J.L. Grebosz, R. Krucken, N. Kurz, Z. Liu, L. Maier, F. Nowacki, S. Pietri, Z. Podolyak, K. Sieja, K. Steiger, K. Straub, H. Weick, H.-J. Wollersheim, P.J. Woods, N. Al-Dahan, N. Alkhomashi, A. Atac, A. Blazhev, N.F. Braun, I.T. Celikovic, T. Davinson, I. Dillmann, C. Domingo-Pardo, P.C. Doornenbal, G. de France, G.F. Farrelly, F. Farinon, N. Goel, T.C. Habermann, R. Hoischen, R. Janik, M. Karny, A. Kaakas, I.M. Kojouharov, T. Kroll, Y. Litvinov, S. Myalski, F. Nebel, S. Nishimura, C. Nociforo, J. Nyberg, A.R. Parikh, A. Prochazka, P.H. Regan, C. Rigollet, H. Schaffner, C. Scheidenberger, S. Schwertel, P.-A. Soderstrom, S.J. Steer, A. Stolz, P. Strmen, Superaligned gamow-teller decay of the doubly magic nucleus ^{100}Sn . Nature **486**(7403), 341–345 (2012). <https://doi.org/10.1038/nature11116>
- D.E.M. Hoff, A.M. Rogers, S.M. Wang, P.C. Bender, K. Brandenburg, K. Childers, J.A. Clark, A.C. Dombos, E.R. Doucet, S. Jin, R. Lewis, S.N. Liddick, C.J. Lister, Z. Meisel, C. Morse, W. Nazarewicz, H. Schatz, K. Schmidt, D. Soltész, S.K. Subedi, S. Waniganethi, Mirror-symmetry violation in bound nuclear ground states. Nature **580**(7801), 52–55 (2020). <https://doi.org/10.1038/s41586-020-2123-1>
- S. Hofmann, W. Reisdorf, G. Münzenberg, F.P. Hessberger, J.R.H. Schneider, P. Armbruster, Proton radioactivity of ^{151}Lu . Z. Phys. **A305**, 111 (1982)
- ISAC www.triumf.ca/research-program/research-facilities/isac-facilities
- ISOLDE <https://isolde.cern/isolde-facility>
- M. Ito, Cluster Thomas-Ehrman shift in ^{10}Be - ^{10}C . EPJ Web of Conferences **117**, 06014 (2016). <https://doi.org/10.1051/epjconf/201611706014>
<https://doi.org/10.1051/epjconf/201611706014>
- K.P. Jackson, C.U. Cardinal, H.C. Evans, N.A. Jelley, J. Cerny, ^{53}mCo : A proton-unstable isomer. Physics Letters B **33**(4), 281–283 (1970). [https://doi.org/10.1016/0370-2693\(70\)90269-8](https://doi.org/10.1016/0370-2693(70)90269-8)
<https://www.sciencedirect.com/science/article/pii/0370269370902698>
- Ł. Janiak, N. Sokołowska, A.A. Bezbakh, A.A. Ciemny, H. Czyrkowski, R. Dąbrowski, W. Dominik, A.S. Fomichev, M.S. Golovkov, A.V. Gorshkov, Z. Janas, G. Kamiński, A.G. Knyazev, S.A. Krupko, M. Kuich, C. Mazzocchi, M. Mentel, M. Pfützner, P. Pluci

- ński, M. Pomorski, R.S. Slepniev, B. Zalewski, β -delayed proton emission from ^{26}P and ^{27}S . *Phys. Rev. C* **95**, 034315 (2017). <https://doi.org/10.1103/PhysRevC.95.034315>. <https://link.aps.org/doi/10.1103/PhysRevC.95.034315>
- B. Jonson, K. Riisager, Beta-decay of exotic nuclei. *Nuclear Physics A* **693**(1), 77–89 (2001). *Radioactive Nuclear Beams*. [https://doi.org/10.1016/S0375-9474\(00\)00560-1](https://doi.org/10.1016/S0375-9474(00)00560-1). <https://www.sciencedirect.com/science/article/pii/S0375947400005601>
- R. Kanungo, M. Chiba, S. Adhikari, D. Fang, N. Iwasa, K. Kimura, K. Maeda, S. Nishimura, Y. Ogawa, T. Ohnishi, A. Ozawa, C. Samanta, T. Suda, T. Suzuki, Q. Wang, C. Wu, Y. Yamaguchi, K. Yamada, A. Yoshida, T. Zheng, I. Tanihata, Possibility of a two-proton halo in ^{17}Ne . *Physics Letters B* **571**(1), 21–28 (2003). <https://doi.org/10.1016/j.physletb.2003.07.050>. <https://www.sciencedirect.com/science/article/pii/S0370269303011031>
- M. Karny, R.K. Grzywacz, J.C. Batchelder, C.R. Bingham, C.J. Gross, K. Hagino, J.H. Hamilton, Z. Janas, W.D. Kulp, J.W. McConnell, M. Momayezi, A. Piechaczek, K.P. Rykaczewski, P.A. Semmes, M.N. Tantawy, J.A. Winger, C.H. Yu, E.F. Zganjar, Fine structure in proton emission from ^{145}Tm discovered with digital signal processing. *Phys. Rev. Lett.* **90**(1), 012502 (2003). <https://doi.org/10.1103/PhysRevLett.90.012502>
- G.J. KeKelis, M.S. Zisman, D.K. Scott, R. Jahn, D.J. Vieira, J. Cerny, F. Ajzenberg-Selove, Masses of the unbound nuclei ^{16}Ne , ^{15}F , and ^{12}O . *Phys. Rev. C* **17**, 1929–1938 (1978). <https://doi.org/10.1103/PhysRevC.17.1929>. <https://link.aps.org/doi/10.1103/PhysRevC.17.1929>
- A.R.L. Kennington, G. Lotay, D.T. Doherty, D. Seweryniak, C. Andreoiu, K. Auranen, M.P. Carpenter, W.N. Catford, C.M. Deibel, K. Hadyńska-Klęk, S. Hallam, D. Hoff, T. Huang, R.V.F. Janssens, S. Jazrawi, J. José, F.G. Kondev, T. Lauritsen, J. Li, A.M. Rogers, J. Saiz, G. Savard, S. Stolze, G.L. Wilson, S. Zhu, Level structure of the $T_z = -1$ nucleus ^{34}Ar and its relevance for nucleosynthesis in one novae. *Phys. Rev. C* **103**, 035805 (2021). <https://doi.org/10.1103/PhysRevC.103.035805>. <https://link.aps.org/doi/10.1103/PhysRevC.103.035805>
- O. Klepper, T. Batsch, S. Hofmann, R. Kirchner, W. Kurcewicz, W. Reisdorf, E. Roeckl, D. Schardt, G. Nyman, Direct and beta-delayed proton decay of very neutron-deficient rare-earth isotopes produced in the reaction $^{58}\text{Ni} + ^{92}\text{Mo}$. *Z. Phys. A* **305**, 125 (1982)
- G.T. Koldste, B. Blank, M.J.G. Borge, J.A. Briz, M. Carmona-Gallardo, L.M. Fraile, H.O.U. Fynbo, J. Giovinazzo, J.G. Johansen, A. Jokinen, B. Jonson, T. Kurturkian-Nieto, J.H. Kusk, T. Nilsson, A. Perea, V. Pesudo, E. Picado, K. Riisager, A. Saastamoinen, O. Tengblad, J.-C. Thomas, J. Van de Walle, Relative proton and γ widths of astrophysically important states in ^{30}S studied in the β -delayed decay of ^{31}Ar . *Phys. Rev. C* **87**, 055808 (2013). <https://doi.org/10.1103/PhysRevC.87.055808>. <https://link.aps.org/doi/10.1103/PhysRevC.87.055808>
- G.T. Koldste, B. Blank, M.J.G. Borge, J.A. Briz, M. Carmona-Gallardo, L.M. Fraile, H.O.U. Fynbo, J. Giovinazzo, B.D. Grann, J.G. Johansen, A. Jokinen, B. Jonson, T. Kurturkian-Nieto, J.H. Kusk, T. Nilsson, A. Perea, V. Pesudo, E. Picado, K. Riisager, A. Saastamoinen, O. Tengblad, J.-C. Thomas, J. Van de Walle, Multiparticle emission in the decay of ^{31}Ar . *Phys. Rev. C* **89**, 064315 (2014a). <https://doi.org/10.1103/PhysRevC.89.064315>. <https://link.aps.org/doi/10.1103/PhysRevC.89.064315>
- G.T. Koldste, B. Blank, M.J.G. Borge, J.A. Briz, M. Carmona-Gallardo, L.M. Fraile, H.O.U. Fynbo, J. Giovinazzo, J.G. Johansen, A. Jokinen, B. Jonson, T. Kurturkian-Nieto, T. Nilsson, A. Perea, V. Pesudo, E. Picado, K. Riisager, A. Saastamoinen, O. Tengblad, J.-C. Thomas, J. Van de Walle, Sizeable beta-strength in ^{31}Ar ($\beta, 3p$) decay. *Physics Letters B* **737**, 383–387 (2014b). <https://doi.org/10.1016/j.physletb.2014.09.015>. <https://www.sciencedirect.com/science/article/pii/S0370269314006650>
- R.A. Kryger, A. Azhari, M. Hellström, J.H. Kelley, T. Kubo, R. Pfaff, E. Ramakrishnan, B.M. Sherrill, M. Thoennessen, S. Yokoyama, R.J. Charity, J. Dempsey, A. Kirov, N. Robertson, D.G. Sarantites, L.G. Sobotka, J.A. Winger, Two-proton emission from the ground state of ^{12}O . *Phys. Rev. Lett.* **74**, 860–863 (1995). <https://doi.org/10.1103/PhysRevLett.74.860>. <https://link.aps.org/doi/10.1103/PhysRevLett.74.860>

- A. Kubiela, H. Suzuki, O.B. Tarasov, M. Pfützner, D.-S. Ahn, H. Baba, A. Bezbakh, A.A. Ciemny, W. Dominik, N. Fukuda, A. Giska, R. Grzywacz, Y. Ichikawa, Z. Janas, L. Janiak, G. Kamiński, K. Kawata, T. Kubo, M. Madurga, C. Mazzocchi, H. Nishibata, M. Pomorski, Y. Shimizu, N. Sokołowska, D. Suzuki, P. Szymkiewicz, A. Świercz, M. Tajima, A. Takamine, H. Takeda, Y. Takeuchi, C.R. Thornsberry, H. Ueno, H. Yamazaki, R. Yokoyama, K. Yoshida, Production of the most neutron-deficient Zn isotopes by projectile fragmentation of ^{78}Kr . *Phys. Rev. C* **104**, 064610 (2021). <https://doi.org/10.1103/PhysRevC.104.064610>
<https://link.aps.org/doi/10.1103/PhysRevC.104.064610>
- C. Langer, O. Lepyoshkina, Y. Aksyutina, T. Aumann, S.B. Novo, J. Benlliure, K. Boretzky, M. Chartier, D. Cortina, U.D. Pramanik, O. Ershova, H. Geissel, R. Gernhäuser, M. Heil, G. Ickert, H.T. Johansson, B. Jonson, A. Kelić-Heil, A. Klimkiewicz, J.V. Kratz, R. Krücken, R. Kulessa, K. Larsson, T. Le Bleis, R. Lemmon, K. Mahata, J. Marganiec, T. Nilsson, V. Panin, R. Plag, W. Prokopowicz, R. Reifarth, V. Ricciardi, D.M. Rossi, S. Schwertel, H. Simon, K. Sümmerer, B. Streicher, J. Taylor, J.R. Vignote, F. Wamers, C. Wimmer, P.Z. Wu, Thermonuclear reaction $^{30}\text{S}(p,\gamma)^{31}\text{Cl}$ studied via Coulomb breakup of ^{31}Cl . *Phys. Rev. C* **89**, 035806 (2014). <https://doi.org/10.1103/PhysRevC.89.035806>
<https://link.aps.org/doi/10.1103/PhysRevC.89.035806>
- J. Lee, X.X. Xu, K. Kaneko, Y. Sun, C.J. Lin, L.J. Sun, P.F. Liang, Z.H. Li, J. Li, H.Y. Wu, D.Q. Fang, J.S. Wang, Y.Y. Yang, C.X. Yuan, Y.H. Lam, Y.T. Wang, K. Wang, J.G. Wang, J.B. Ma, J.J. Liu, P.J. Li, Q.Q. Zhao, L. Yang, N.R. Ma, D.X. Wang, F.P. Zhong, S.H. Zhong, F. Yang, H.M. Jia, P.W. Wen, M. Pan, H.L. Zang, X. Wang, C.G. Wu, D.W. Luo, H.W. Wang, C. Li, C.Z. Shi, M.W. Nie, X.F. Li, H. Li, P. Ma, Q. Hu, G.Z. Shi, S.L. Jin, M.R. Huang, Z. Bai, Y.J. Zhou, W.H. Ma, F.F. Duan, S.Y. Jin, Q.R. Gao, X.H. Zhou, Z.G. Hu, M. Wang, M.L. Liu, R.F. Chen, X.W. Ma, Large isospin asymmetry in $^{22}\text{Si}/^{22}\text{O}$ mirror Gamow-Teller transitions reveals the halo structure of ^{22}Al . *Phys. Rev. Lett.* **125**, 192503 (2020). <https://doi.org/10.1103/PhysRevLett.125.192503>
<https://link.aps.org/doi/10.1103/PhysRevLett.125.192503>
- M. Leino, J. Äystö, T. Enqvist, P. Heikkinen, A. Jokinen, M. Nurmi, A. Ostrowski, W.H. Trzaska, J. Uusitalo, K. Eskola, P. Armbruster, V. Ninov, Gas-filled recoil separator for studies of heavy elements. *Nuclear Instruments and Methods in Physics Research Section B: Beam Interactions with Materials and Atoms* **99**(1), 653–656 (1995). Application of Accelerators in Research and Industry '94. [https://doi.org/10.1016/0168-583X\(94\)00573-7](https://doi.org/10.1016/0168-583X(94)00573-7)
<https://www.sciencedirect.com/science/article/pii/0168583X94005737>
- S.M. Lenzi, A. Poves, A.O. Macchiavelli, Isospin symmetry breaking in the mirror pair $^{73}\text{Sr} - ^{73}\text{Br}$. *Phys. Rev. C* **102**, 031302 (2020). <https://doi.org/10.1103/PhysRevC.102.031302>
<https://link.aps.org/doi/10.1103/PhysRevC.102.031302>
- M. Lewitowicz, R. Anne, G. Auger, D. Bazin, C. Borcea, V. Borrel, J.M. Corre, T. Dorfler, A. Fomichev, R. Grzywacz, D. Guillemaud-Mueller, R. Hue, M. Huyse, Z. Janas, H. Keller, S. Lukyanov, A.C. Mueller, Y. Penionzhkevich, M. Pfützner, F. Pougheon, K. Rykaczewski, M.G. Saint-Laurent, K. Schmidt, W.D. Schmidt-Ott, O. Sorlin, J. Szerypo, O. Tarasov, J. Wauters, J. Żylicz, Identification of ^{100}Sn and others proton drip-line nuclei in the reaction $^{112}\text{Sn}(63 \text{ MeV}/\text{nucl.})+\text{natNi}$. *Nuclear Physics A* **588**(1), 197–202 (1995). Proceedings of the Fifth International Symposium on Physics of Unstable Nuclei. [https://doi.org/10.1016/0375-9474\(95\)00139-R](https://doi.org/10.1016/0375-9474(95)00139-R)
<https://www.sciencedirect.com/science/article/pii/037594749500139R>
- S.N. Liddick, R. Grzywacz, C. Mazzocchi, R.D. Page, K.P. Rykaczewski, J.C. Batchelder, C.R. Bingham, I.G. Darby, G. Drafta, C. Goodin, C.J. Gross, J.H. Hamilton, A.A. Hecht, J.K. Hwang, S. Ilyushkin, D.T. Joss, A. Korgul, W. Królas, K. Lagergren, K. Li, M.N. Tantawy, J. Thomson, J.A. Winger, Discovery of ^{109}Xe and ^{105}Te : Superallowed α decay near doubly magic ^{100}Sn . *Phys. Rev. Lett.* **97**, 082501 (2006). <https://doi.org/10.1103/PhysRevLett.97.082501>
<https://link.aps.org/doi/10.1103/PhysRevLett.97.082501>
- A.A. Lis, C. Mazzocchi, W. Dominik, Z. Janas, M. Pfützner, M. Pomorski, L. Acosta, S. Baraeva, E. Casarejos, J. Duéñas-Díaz, V. Dunin, J.M. Espino, A. Estrade, F. Farinon, A. Fomichev, H. Geissel, A. Gorshkov, G. Kamiński, O. Kiselev, R. Knöbel, S. Krupko, M. Kuich, Y.A.

- Litvinov, G. Marquinez-Durán, I. Martel, I. Mukha, C. Nociforo, A.K. Ordúz, S. Pietri, A. Prochazka, A.M. Sánchez-Benítez, H. Simon, B. Sitar, R. Slepnev, M. Stanoiu, P. Strmen, I. Szarka, M. Takechi, Y. Tanaka, H. Weick, J.S. Winfield, β -delayed three-proton decay of ^{31}Ar . *Phys. Rev. C* **91**, 064309 (2015). <https://doi.org/10.1103/PhysRevC.91.064309>. <https://link.aps.org/doi/10.1103/PhysRevC.91.064309>
- D. Lubos, J. Park, T. Faestermann, R. Gernhäuser, R. Krücken, M. Lewitowicz, S. Nishimura, H. Sakurai, D.S. Ahn, H. Baba, B. Blank, A. Blazhev, P. Boutachkov, F. Browne, I. Čeliković, G. de France, P. Doornenbal, Y. Fang, N. Fukuda, J. Giovinazzo, N. Goel, M. Górska, S. Ilieva, N. Inabe, T. Isobe, A. Jungclaus, D. Kameda, Y.K. Kim, I. Kojouharov, T. Kubo, N. Kurz, Y.K. Kwon, G. Lorusso, K. Moschner, D. Murai, I. Nishizuka, Z. Patel, M.M. Rajabali, S. Rice, H. Schaffner, Y. Shimizu, L. Sinclair, P.-A. Söderström, K. Steiger, T. Sumikama, H. Suzuki, H. Takeda, Z. Wang, N. Warr, H. Watanabe, J. Wu, Z. Xu, Improved value for the Gamow-Teller strength of the ^{100}Sn beta decay. *Phys. Rev. Lett.* **122**, 222502 (2019). <https://doi.org/10.1103/PhysRevLett.122.222502>. <https://link.aps.org/doi/10.1103/PhysRevLett.122.222502>
- M.V. Lund, M.J.G. Borge, J.A. Briz, J. Cederkall, H.O.U. Fynbo, J.H. Jensen, B. Jonsson, K.L. Laursen, T. Nilsson, A. Perea, V. Pesudo, K. Riisager, O. Tengblad, Systematic trends in beta-delayed particle emitting nuclei: The case of $\beta p \alpha$ emission from ^{21}Mg . *Physics Letters B* **750**, 356–359 (2015). <https://doi.org/10.1016/j.physletb.2015.09.044>. <https://www.sciencedirect.com/science/article/pii/S0370269315007194>
- R.D. Macfarlane, A. Siivola, New region of alpha radioactivity. *Phys. Rev. Lett.* **14**, 114–115 (1965). <https://doi.org/10.1103/PhysRevLett.14.114>. <https://link.aps.org/doi/10.1103/PhysRevLett.14.114>
- A. Magilligan, B.A. Brown, New isospin-breaking “usd” hamiltonians for the sd shell. *Phys. Rev. C* **101**, 064312 (2020). <https://doi.org/10.1103/PhysRevC.101.064312>. <https://link.aps.org/doi/10.1103/PhysRevC.101.064312>
- C. Mazzocchi, Z. Janas, L. Batist, V. Belleguic, J. Döring, M. Gierlik, M. Kapica, R. Kirchner, G.A. Lalazissis, H. Mahmud, E. Roeckl, P. Ring, K. Schmidt, P.J. Woods, J. Żylicz, Alpha decay of ^{114}Ba . *Physics Letters B* **532**(1), 29–36 (2002). [https://doi.org/10.1016/S0370-2693\(02\)01543-5](https://doi.org/10.1016/S0370-2693(02)01543-5). <https://www.sciencedirect.com/science/article/pii/S0370269302015435>
- C. Mazzocchi, R. Grzywacz, S.N. Liddick, K.P. Rykaczewski, H. Schatz, J.C. Batchelder, C.R. Bingham, C.J. Gross, J.H. Hamilton, J.K. Hwang, S. Ilyushkin, A. Korgul, W. Królas, K. Li, R.D. Page, D. Simpson, J.A. Winger, α decay of ^{109}I and its implications for the proton decay of ^{105}Sb and the astrophysical rapid proton-capture process. *Phys. Rev. Lett.* **98**, 212501 (2007). <https://doi.org/10.1103/PhysRevLett.98.212501>. <https://link.aps.org/doi/10.1103/PhysRevLett.98.212501>
- K. Miernik, W. Dominik, Z. Janas, M. Pfützner, C.R. Bingham, H. Czyrkowski, M. Ćwiok, I.G. Darby, R. Dąbrowski, T. Ginter, R. Grzywacz, M. Karny, A. Korgul, W. Kuśmierz, S.N. Liddick, M. Rajabali, K. Rykaczewski, A. Stolz, First observation of β -delayed three-proton emission in ^{45}Fe . *Phys. Rev. C* **76**, 041304 (2007a). <https://doi.org/10.1103/PhysRevC.76.041304>. <https://link.aps.org/doi/10.1103/PhysRevC.76.041304>
- K. Miernik, W. Dominik, Z. Janas, M. Pfützner, L. Grigorenko, C.R. Bingham, H. Czyrkowski, M. Ćwiok, I.G. Darby, R. Dąbrowski, T. Ginter, R. Grzywacz, M. Karny, A. Korgul, W. Kuśmierz, S.N. Liddick, M. Rajabali, K. Rykaczewski, A. Stolz, Two-proton correlations in the decay of ^{45}Fe . *Phys. Rev. Lett.* **99**, 192501 (2007b). <https://doi.org/10.1103/PhysRevLett.99.192501>. <https://link.aps.org/doi/10.1103/PhysRevLett.99.192501>
- T. Minamisono, T. Ohtsubo, I. Minami, S. Fukuda, A. Kitagawa, M. Fukuda, K. Matsuta, Y. Nojiri, S. Takeda, H. Sagawa, H. Kitagawa, Proton halo of ^8B disclosed by its giant quadrupole moment. *Phys. Rev. Lett.* **69**, 2058–2061 (1992). <https://doi.org/10.1103/PhysRevLett.69.2058>. <https://link.aps.org/doi/10.1103/PhysRevLett.69.2058>
- R. Morlock, R. Kunz, A. Mayer, M. Jaeger, A. Müller, J.W. Hammer, P. Mohr, H. Oberhammer, G. Staudt, V. Kölle, Halo properties of the first $1/2^+$ state in ^{17}F from the $^{16}\text{O}(p, \gamma)^{17}\text{F}$ reaction. *Phys. Rev. Lett.* **79**, 3837–3840 (1997). <https://doi.org/10.1103/PhysRevLett.79.3837>. <https://link.aps.org/doi/10.1103/PhysRevLett.79.3837>

- D.J. Morrissey, B.M. Sherrill, M. Steiner, A. Stolz, I. Wiedenhoever, Commissioning the A1900 projectile fragment separator. *Nuclear Instruments and Methods in Physics Research Section B: Beam Interactions with Materials and Atoms* **204**, 90–96 (2003). 14th International Conference on Electromagnetic Isotope Separators and Techniques Related to their Applications. [https://doi.org/10.1016/S0168-583X\(02\)01895-5](https://doi.org/10.1016/S0168-583X(02)01895-5). <https://www.sciencedirect.com/science/article/pii/S0168583X02018955>
- A.C. Mueller, R. Anne, Production of and studies with secondary radioactive ion beams at LISE. *Nuclear Instruments and Methods in Physics Research Section B: Beam Interactions with Materials and Atoms* **56-57**, 559–563 (1991). [https://doi.org/10.1016/0168-583X\(91\)96095-3](https://doi.org/10.1016/0168-583X(91)96095-3). <https://www.sciencedirect.com/science/article/pii/0168583X91960953>
- I. Mukha, L.V. Grigorenko, X. Xu, L. Acosta, E. Casarejos, A.A. Ciemny, W. Dominik, J. Duéñas-Díaz, V. Dunin, J.M. Espino, A. Estradé, F. Farinon, A. Fomichev, H. Geissel, T.A. Golubkova, A. Gorshkov, Z. Janas, G. Kamiński, O. Kiselev, R. Knöbel, S. Krupko, M. Kuich, Y.A. Litvinov, G. Marquinez-Durán, I. Martel, C. Mazzocchi, C. Nociforo, A.K. Ordúz, M. Pfützner, S. Pietri, M. Pomorski, A. Prochazka, S. Rymzhanova, A.M. Sánchez-Benítez, C. Scheidenberger, P. Sharov, H. Simon, B. Sitar, R. Slepnev, M. Stanoiu, P. Strmen, I. Szarka, M. Takechi, Y.K. Tanaka, H. Weick, M. Winkler, J.S. Winfield, M.V. Zhukov, Observation and spectroscopy of new proton-unbound isotopes ^{30}Ar and ^{29}Cl : An interplay of prompt two-proton and sequential decay. *Phys. Rev. Lett.* **115**, 202501 (2015). <https://doi.org/10.1103/PhysRevLett.115.202501>. <https://link.aps.org/doi/10.1103/PhysRevLett.115.202501>
- I. Mukha, L.V. Grigorenko, D. Kostyleva, L. Acosta, E. Casarejos, A.A. Ciemny, W. Dominik, J.A. Dueñas, V. Dunin, J.M. Espino, A. Estradé, F. Farinon, A. Fomichev, H. Geissel, A. Gorshkov, Z. Janas, G. Kamiński, O. Kiselev, R. Knöbel, S. Krupko, M. Kuich, Y.A. Litvinov, G. Marquinez-Durán, I. Martel, C. Mazzocchi, C. Nociforo, A.K. Ordúz, M. Pfützner, S. Pietri, M. Pomorski, A. Prochazka, S. Rymzhanova, A.M. Sánchez-Benítez, C. Scheidenberger, P. Sharov, H. Simon, B. Sitar, R. Slepnev, M. Stanoiu, P. Strmen, I. Szarka, M. Takechi, Y.K. Tanaka, H. Weick, M. Winkler, J.S. Winfield, X. Xu, M.V. Zhukov, Deep excursion beyond the proton dripline. i. Argon and chlorine isotope chains. *Phys. Rev. C* **98**, 064308 (2018). <https://doi.org/10.1103/PhysRevC.98.064308>. <https://link.aps.org/doi/10.1103/PhysRevC.98.064308>
- H. Nakada, T. Otsuka, E2 properties of nuclei far from stability and the proton-halo problem of ^8B . *Phys. Rev. C* **49**, 886–894 (1994). <https://doi.org/10.1103/PhysRevC.49.886>. <https://link.aps.org/doi/10.1103/PhysRevC.49.886>
- M. Nakao, H. Umehara, S. Ebata, M. Ito, Cluster Thomas-Ehrman effect in mirror nuclei. *Phys. Rev. C* **98**, 054318 (2018). <https://doi.org/10.1103/PhysRevC.98.054318>. <https://link.aps.org/doi/10.1103/PhysRevC.98.054318>
- A. Navin, D. Bazin, B.A. Brown, B. Davids, G. Gervais, T. Glasmacher, K. Govaert, P.G. Hansen, M. Hellström, R.W. Ibbotson, V. Maddalena, B. Pritychenko, H. Scheit, B.M. Sherrill, M. Steiner, J.A. Tostevin, J. Yurkon, Spectroscopy of radioactive beams from single-nucleon knockout reactions: Application to the sd shell nuclei ^{25}Al and $^{26,27,28}\text{P}$. *Phys. Rev. Lett.* **81**, 5089–5092 (1998). <https://doi.org/10.1103/PhysRevLett.81.5089>. <https://link.aps.org/doi/10.1103/PhysRevLett.81.5089>
- T. Neff, H. Feldmeier, Clustering and other exotic phenomena in nuclei. *The European Physical Journal Special Topics* **156**(1), 69–92 (2008). <https://doi.org/10.1140/epjst/e2008-00609-y>. <https://doi.org/10.1140/epjst/e2008-00609-y>
- L. Neufcourt, Y. Cao, S. Giuliani, W. Nazarewicz, E. Olsen, O.B. Tarasov, Beyond the proton drip line: Bayesian analysis of proton-emitting nuclei. *Phys. Rev. C* **101**, 014319 (2020a). <https://doi.org/10.1103/PhysRevC.101.014319>. <https://link.aps.org/doi/10.1103/PhysRevC.101.014319>
- L. Neufcourt, Y. Cao, S.A. Giuliani, W. Nazarewicz, E. Olsen, O.B. Tarasov, Quantified limits of the nuclear landscape. *Phys. Rev. C* **101**, 044307 (2020b). <https://doi.org/10.1103/PhysRevC.101.044307>. <https://link.aps.org/doi/10.1103/PhysRevC.101.044307>

- E. Olsen, M. Pfützner, N. Birge, M. Brown, W. Nazarewicz, A. Perhac, Erratum: Landscape of two-proton radioactivity [Phys. Rev. Lett. 110, 222501 (2013)]. Phys. Rev. Lett. **111**, 139903 (2013a). <https://doi.org/10.1103/PhysRevLett.111.139903>. <https://link.aps.org/doi/10.1103/PhysRevLett.111.139903>
- E. Olsen, M. Pfützner, N. Birge, M. Brown, W. Nazarewicz, A. Perhac, Landscape of two-proton radioactivity. Phys. Rev. Lett. **110**, 222501 (2013b). <https://doi.org/10.1103/PhysRevLett.110.222501>. <https://link.aps.org/doi/10.1103/PhysRevLett.110.222501>
- T. Otsuka, A. Gade, O. Sorlin, T. Suzuki, Y. Utsuno, Evolution of shell structure in exotic nuclei. Rev. Mod. Phys. **92**, 015002 (2020). <https://doi.org/10.1103/RevModPhys.92.015002>. <https://link.aps.org/doi/10.1103/RevModPhys.92.015002>
- A. Ozawa, M. Fujimaki, S. Fukuda, S. Ito, T. Kobayashi, S. Momota, T. Suzuki, I. Tanihata, K. Yoshida, G. Kraus, G. Münzenberg, Measurement of the β -decay branching ratio of into the first excited state of ^{17}F . Journal of Physics G: Nuclear and Particle Physics **24**(1), 143–150 (1998). <https://doi.org/10.1088/0954-3899/24/1/018>. <https://doi.org/10.1088/0954-3899/24/1/018>
- D. Pérez-Loureiro, C. Wrede, M.B. Bennett, S.N. Liddick, A. Bowe, B.A. Brown, A.A. Chen, K.A. Chipps, N. Cooper, D. Irvine, E. McNeice, F. Montes, F. Naqvi, R. Ortez, S.D. Pain, J. Pereira, C.J. Prokop, J. Quaglia, S.J. Quinn, J. Sakstrup, M. Santia, S.B. Schwartz, S. Shanab, A. Simon, A. Spyrou, E. Thiagalingam, β -delayed γ decay of ^{26}P : Possible evidence of a proton halo. Phys. Rev. C **93**, 064320 (2016). <https://doi.org/10.1103/PhysRevC.93.064320>. <https://link.aps.org/doi/10.1103/PhysRevC.93.064320>
- M. Pfützner, E. Badura, C. Bingham, B. Blank, M. Chartier, H. Geissel, J. Giovinazzo, L.V. Grigorenko, K. Grzywacz, M. Hellström, Z. Janas, J. Kurcewicz, A.S. Lalleman, C. Mazzocchi, I. Mukha, G. Münzenberg, C. Plettner, E. Roeckl, K.P. Rykaczewski, K. Schmidt, R.S. Simon, M. Stanoiu, J.-C. Thomas, First evidence for the two-proton decay of ^{45}Fe . Eur. Phys. J. A **14**, 279 (2002). <https://doi-org.ezproxy.cern.ch/10.1140/epja/i2002-10033-9>
- M. Pfützner, M. Karny, L.V. Grigorenko, K. Riisager, Radioactive decays at limits of nuclear stability. Rev. Mod. Phys. **84**, 567–619 (2012). <https://doi.org/10.1103/RevModPhys.84.567>. <https://link.aps.org/doi/10.1103/RevModPhys.84.567>
- M. Pomorski, K. Miernik, W. Dominik, Z. Janas, M. Pfützner, C.R. Bingham, H. Czyrkowski, M. Ćwiok, I.G. Darby, R. Dąbrowski, T. Ginter, R. Grzywacz, M. Karny, A. Korgul, W. Kuśmierz, S.N. Liddick, M. Rajabali, K. Rykaczewski, A. Stolz, β -delayed proton emission branches in ^{43}Cr . Phys. Rev. C **83**, 014306 (2011a). <https://doi.org/10.1103/PhysRevC.83.014306>. <https://link.aps.org/doi/10.1103/PhysRevC.83.014306>
- M. Pomorski, M. Pfützner, W. Dominik, R. Grzywacz, T. Baumann, J.S. Berryman, H. Czyrkowski, R. Dąbrowski, T. Ginter, J. Johnson, G. Kamiński, A. Kuźniak, N. Larson, S.N. Liddick, M. Madurga, C. Mazzocchi, S. Mianowski, K. Miernik, D. Miller, S. Paulauskas, J. Pereira, K.P. Rykaczewski, A. Stolz, S. Suchyta, First observation of two-proton radioactivity in ^{48}Ni . Phys. Rev. C **83**, 061303 (2011b). <https://doi.org/10.1103/PhysRevC.83.061303>. <https://link.aps.org/doi/10.1103/PhysRevC.83.061303>
- M. Pomorski, M. Pfützner, W. Dominik, R. Grzywacz, A. Stolz, T. Baumann, J.S. Berryman, H. Czyrkowski, R. Dąbrowski, A. Fijałkowska, T. Ginter, J. Johnson, G. Kamiński, N. Larson, S.N. Liddick, M. Madurga, C. Mazzocchi, S. Mianowski, K. Miernik, D. Miller, S. Paulauskas, J. Pereira, K.P. Rykaczewski, S. Suchyta, Proton spectroscopy of ^{48}Ni , ^{46}Fe , and ^{44}Cr . Phys. Rev. C **90**, 014311 (2014). <https://doi.org/10.1103/PhysRevC.90.014311>. <https://link.aps.org/doi/10.1103/PhysRevC.90.014311>
- S.E. Rutherford, A.B. Wood, XLIII. Long-range alpha particles from Thorium. The London, Edinburgh, and Dublin Philosophical Magazine and Journal of Science **31**(184), 379–386 (1916). <https://doi.org/10.1080/14786440408635510>. <https://doi.org/10.1080/14786440408635510>
- H. Sakurai, RI beam factory project at RIKEN. Nuclear Physics A **805**(1–4), 526–532 (2008). INPC 2007 - Proceedings of the 23rd International Nuclear Physics Conference. <https://doi.org/DOI:10.1016/j.nuclphysa.2008.02.291>

- P. Sarriguren, Stellar weak decay rates in neutron-deficient medium-mass nuclei. *Phys. Rev. C* **83**, 025801 (2011). <https://doi.org/10.1103/PhysRevC.83.025801>. <https://link.aps.org/doi/10.1103/PhysRevC.83.025801>
- H. Schatz, A. Aprahamian, J. Görres, M. Wiescher, T. Rauscher, J.F. Rembges, F.-K. Thielemann, B. Pfeiffer, P. Möller, K.-L. Kratz, H. Herndl, B.A. Brown, H. Rebel, *rp*-process nucleosynthesis at extreme temperature and density conditions. *Physics Reports* **294**(4), 167–263 (1998). [https://doi.org/DOI:10.1016/S0370-1573\(97\)00048-3](https://doi.org/DOI:10.1016/S0370-1573(97)00048-3)
- H. Schatz, A. Aprahamian, V. Barnard, L. Bildsten, A. Cumming, M. Ouellette, T. Rauscher, F.-K. Thielemann, M. Wiescher, End point of the *rp* process on accreting neutron stars. *Phys. Rev. Lett.* **86**, 3471–3474 (2001). <https://doi.org/10.1103/PhysRevLett.86.3471>. <https://link.aps.org/doi/10.1103/PhysRevLett.86.3471>
- R. Schneider, T. Faestermann, J. Friese, R. Gernhauser, H. Geissel, H. Gilg, F. Heine, J. Homolka, P. Kienle, H.-J. Korner, G. Munzenberg, J. Reinhold, K. Summerer, K. Zeitelhack, Production, identification, and half-life measurement of ^{100}Sn . *Nuclear Physics A* **588**(1), 191–196 (1995). Proceedings of the Fifth International Symposium on Physics of Unstable Nuclei. [https://doi.org/10.1016/0375-9474\(95\)00138-Q](https://doi.org/10.1016/0375-9474(95)00138-Q). <https://www.sciencedirect.com/science/article/pii/037594749500138Q>
- W. Schwab, H. Geissel, H. Lenske, K.-H. Behr, A. Brünle, K. Burkard, H. Irmich, T. Kobayashi, G. Kraus, A. Magel, G. Münzenberg, F. Nickel, K. Riisager, C. Scheidenberger, B.M. Sherrill, T. Suzuki, B. Voss, Observation of a proton halo in 8B . *Zeitschrift für Physik A Hadrons and Nuclei* **350**(4), 283–284 (1995). <https://doi.org/10.1007/BF01291183>. <https://doi.org/10.1007/BF01291183>
- D. Seweryniak, W.B. Walters, A. Woehr, M. Lipoglavsek, J. Shergur, C.N. Davids, A. Heinz, J.J. Ressler, Population of the 168-keV ($g_{7/2}$) excited state in ^{103}Sn in the α decay of ^{107}Te . *Phys. Rev. C* **66**, 051307 (2002). <https://doi.org/10.1103/PhysRevC.66.051307>. <https://link.aps.org/doi/10.1103/PhysRevC.66.051307>
- D. Seweryniak, K. Starosta, C.N. Davids, S. Gros, A.A. Hecht, N. Hoteling, T.L. Khoo, K. Lagergren, G. Lotay, D. Peterson, A. Robinson, C. Vaman, W.B. Walters, P.J. Woods, S. Zhu, α decay of ^{105}Te . *Phys. Rev. C* **73**, 061301 (2006). <https://doi.org/10.1103/PhysRevC.73.061301>. <https://link.aps.org/doi/10.1103/PhysRevC.73.061301>
- D. Seweryniak, M.P. Carpenter, S. Gros, A.A. Hecht, N. Hoteling, R.V.F. Janssens, T.L. Khoo, T. Lauritsen, C.J. Lister, G. Lotay, D. Peterson, A.P. Robinson, W.B. Walters, X. Wang, P.J. Woods, S. Zhu, Single-neutron states in ^{101}Sn . *Phys. Rev. Lett.* **99**, 022504 (2007). <https://doi.org/10.1103/PhysRevLett.99.022504>. <https://link.aps.org/doi/10.1103/PhysRevLett.99.022504>
- B.M. Sherrill, Future opportunities at the facility for rare isotope beams. *EPJ Web Conf.* **178**, 01001 (2018). <https://doi.org/10.1051/epjconf/201817801001>. <https://doi.org/10.1051/epjconf/201817801001>
- R. Sparta, A. Di Pietro, P. Figuera, O. Tengblad, A.M. Moro, I. Martel, J.P. Fernández-García, J. Lei, L. Acosta, M.J.G. Borge, G. Bruni, J. Cederkäll, T. Davinson, J.D. Ovejas, L.M. Fraile, D. Galaviz, J. Halkjaer Jensen, B. Jonson, M. La Cognata, A. Perea, A.M. Sánchez-Benítez, N. Soić, S. Vinals, Probing proton halo effects in the $8\text{B}+64\text{Zn}$ collision around the Coulomb barrier. *Physics Letters B* **820**, 136477 (2021). <https://doi.org/10.1016/j.physletb.2021.136477>. <https://www.sciencedirect.com/science/article/pii/S0370269321004172>
- L.J. Sun, X.X. Xu, C.J. Lin, J. Lee, S.Q. Hou, C.X. Yuan, Z.H. Li, J. José, J.J. He, J.S. Wang, D.X. Wang, H.Y. Wu, P.F. Liang, Y.Y. Yang, Y.H. Lam, P. Ma, F.F. Duan, Z.H. Gao, Q. Hu, Z. Bai, J.B. Ma, J.G. Wang, F.P. Zhong, C.G. Wu, D.W. Luo, Y. Jiang, Y. Liu, D.S. Hou, R. Li, N.R. Ma, W.H. Ma, G.Z. Shi, G.M. Yu, D. Patel, S.Y. Jin, Y.F. Wang, Y.C. Yu, Q.W. Zhou, P. Wang, L.Y. Hu, X. Wang, H.L. Zang, P.J. Li, Q.Q. Zhao, L. Yang, P.W. Wen, F. Yang, H.M. Jia, G.L. Zhang, M. Pan, X.Y. Wang, H.H. Sun, Z.G. Hu, R.F. Chen, M.L. Liu, W.Q. Yang, Y.M. Zhao, H.Q. Zhang, β -decay spectroscopy of ^{27}S . *Phys. Rev. C* **99**, 064312 (2019). <https://doi.org/10.1103/PhysRevC.99.064312>. <https://link.aps.org/doi/10.1103/PhysRevC.99.064312>

- I. Tanihata, H. Hamagaki, O. Hashimoto, Y. Shida, N. Yoshikawa, K. Sugimoto, O. Yamakawa, T. Kobayashi, N. Takahashi, Measurements of interaction cross sections and nuclear radii in the light p -shell region. *Phys. Rev. Lett.* **55**, 2676–2679 (1985). <https://doi.org/10.1103/PhysRevLett.55.2676>
<https://link.aps.org/doi/10.1103/PhysRevLett.55.2676>
- R.G. Thomas, An analysis of the energy levels of the mirror nuclei, C^{13} and N^{13} . *Phys. Rev.* **88**, 1109–1125 (1952). <https://doi.org/10.1103/PhysRev.88.1109>
<https://link.aps.org/doi/10.1103/PhysRev.88.1109>
- I.J. Thompson, Coupled reaction channels calculations in nuclear physics. *Computer Physics Reports* **7**(4), 167–212 (1988). [https://doi.org/10.1016/0167-7977\(88\)90005-6](https://doi.org/10.1016/0167-7977(88)90005-6)
<https://www.sciencedirect.com/science/article/pii/0167797788900056>
- J.J. Valiente-Dobón, A. Poves, A. Gadea, B. Fernández-Domínguez, Broken mirror symmetry in ^{36}S and ^{36}Ca . *Phys. Rev. C* **98**, 011302 (2018). <https://doi.org/10.1103/PhysRevC.98.011302>
<https://link.aps.org/doi/10.1103/PhysRevC.98.011302>
- K. Varga, R.G. Lovas, R.J. Liotta, Absolute alpha decay width of ^{212}Po in a combined shell and cluster model. *Phys. Rev. Lett.* **69**, 37–40 (1992). <https://doi.org/10.1103/PhysRevLett.69.37>
<https://link.aps.org/doi/10.1103/PhysRevLett.69.37>
- S.M. Wang, N. Michel, W. Nazarewicz, F.R. Xu, Structure and decays of nuclear three-body systems: The Gamow coupled-channel method in Jacobi coordinates. *Phys. Rev. C* **96**, 044307 (2017). <https://doi.org/10.1103/PhysRevC.96.044307>
<https://link.aps.org/doi/10.1103/PhysRevC.96.044307>
- R.E. Warner, J.H. Kelley, P. Zecher, F.D. Becchetti, J.A. Brown, C.L. Carpenter, A. Galonsky, J. Kruse, A. Muthukrishnan, A. Nadasen, R.M. Ronning, P. Schwandt, B.M. Sherrill, J. Wang, J.S. Winfield, Evidence for a proton halo in ^8B : Enhanced total reaction cross sections at 20 to 60 MeV/nucleon. *Phys. Rev. C* **52**, 1166–1170 (1995). <https://doi.org/10.1103/PhysRevC.52.R1166>
<https://link.aps.org/doi/10.1103/PhysRevC.52.R1166>
- T.B. Webb, S.M. Wang, K.W. Brown, R.J. Charity, J.M. Elson, J. Barney, G. Cerizza, Z. Chajecski, J. Estee, D.E.M. Hoff, S.A. Kuvin, W.G. Lynch, J. Manfredi, D. McNeel, P. Morfouace, W. Nazarewicz, C.D. Pruitt, C. Santamaria, J. Smith, L.G. Sobotka, S. Sweany, C.Y. Tsang, M.B. Tsang, A.H. Wuosmaa, Y. Zhang, K. Zhu, First observation of unbound ^{11}O , the mirror of the halo nucleus ^{11}Li . *Phys. Rev. Lett.* **122**, 122501 (2019). <https://doi.org/10.1103/PhysRevLett.122.122501>
<https://link.aps.org/doi/10.1103/PhysRevLett.122.122501>
- D.H. Wilkinson, B.E.F. Macefield, A parametrization of the phase space factor for allowed β -decay. *Nuclear Physics A* **232**(1), 58–92 (1974). [https://doi.org/10.1016/0375-9474\(74\)90645-9](https://doi.org/10.1016/0375-9474(74)90645-9)
<https://www.sciencedirect.com/science/article/pii/0375947474906459>
- Y. Xiao, S. Go, R. Grzywacz, R. Orlandi, A.N. Andreyev, M. Asai, M.A. Bentley, G. de Angelis, C.J. Gross, P. Hausladen, K. Hirose, S. Hofmann, H. Ikezoe, D.G. Jenkins, B. Kindler, R. Léguillon, B. Lommel, H. Makii, C. Mazzocchi, K. Nishio, P. Parkhurst, S.V. Paulauskas, C.M. Petrache, K.P. Rykaczewski, T.K. Sato, J. Smallcombe, A. Toyoshima, K. Tsukada, K. Vaigneur, R. Wadsworth, Search for α decay of ^{104}Te with a novel recoil-decay scintillation detector. *Phys. Rev. C* **100**, 034315 (2019). <https://doi.org/10.1103/PhysRevC.100.034315>
<https://link.aps.org/doi/10.1103/PhysRevC.100.034315>
- Y.B. Zeldovich, On existence of new isotopes of light nuclei and neutron equation of state. *Sov. Phys. JETP* **11**, 812 (1960)
- A.P. Zuker, S.M. Lenzi, G. Martínez-Pinedo, A. Poves, Isobaric multiplet yrast energies and isospin nonconserving forces. *Phys. Rev. Lett.* **89**, 142502 (2002). <https://doi.org/10.1103/PhysRevLett.89.142502>
<https://link.aps.org/doi/10.1103/PhysRevLett.89.142502>